# An assay toolkit for anti-tuberculosis drugs in the hollow fiber system

Fernando Sanz-García[1,6*], Dominique Ndjogou[2], Diana A. Aguilar-Ayala[1], Maxime R. Eveque-Mourroux[2], Ana Benítez[1], Sergio Aznar[1], Nuria Isach-Traver[1], Alfonso Mendoza-Losana[3], Nicolas Willand[2], Ainhoa Lucía[1,4,#], Santiago Ramón-García[1,4,5,*,#] on behalf of the ERA4TB consortium.

[1]Department of Microbiology, University of Zaragoza, C/ Domingo Miral s/n 50009-Zaragoza, Spain

[2]Univ. Lille, Inserm, Institut Pasteur de Lille, U1177 - Drugs and Molecules for Living Systems, F-59000 Lille, France.

[3]Biomedical Sciences and Engineering Laboratory, Bioengineering Department, Universidad Carlos III de Madrid, 28903, Madrid, Spain.

[4]Spanish Network for Research on Respiratory Diseases (CIBERES), Carlos III Health Institute, 28029 Madrid, Spain

[5]Research & Development Agency of Aragón (ARAID) Foundation, Zaragoza, Spain.

[6]Lead contact

#: Equal contribution

*Correspondence: f.sanzg@unizar.es and santiramon@unizar.es

## SUMMARY

The hollow-fiber system for tuberculosis (HFS-TB) is an *in vitro* pharmacokinetic/pharmacodynamic (PKPD) tool qualified by the European Medicines Agency to support anti-TB drug development. It can simulate PK parameters of antimicrobials and feed *in silico* models to inform Phase II/III clinical trials. Yet, its implementation is challenging due to lack of consolidated technical guidelines, such as the compatibility of drugs with the most commonly used types of HFS-TB cartridges. Herein, we uncovered the compatibility of 10 anti-TB drugs alone: bedaquiline, clarithromycin, delamanid, ethambutol, isoniazid, linezolid, moxifloxacin, pretomanid, rifampicin and rifapentine; and a combination: bedaquiline-pretomanid-linezolid. The most hydrophilic compounds were within the compatibility range with all fibers; whereas the lipophilic ones required adjustments to be used in the system. Also, polysulfone and cellulose fibers were the most suitable for the tested drugs. Our data strengthen the importance of these preliminary studies and provide a useful toolkit towards wider HFS-TB implementation.


**Keywords**: hollow-fiber system, tuberculosis, pharmacokinetics, standardization, cartridge compatibility, lipophilicity, BPaL.

## INTRODUCTION

Upon the first report in 2004 [1], the hollow-fiber system for tuberculosis (HFS-TB) was subjected to formal evaluation by the European Medicines Agency (EMA), leading to endorsement for TB drug development in 2015 [2,3] and, subsequently, by the Food and Drug Administration (FDA) [4]. This preclinical model permits exposing a growing culture of *Mycobacterium tuberculosis* to any simulated antibiotic dose by mimicking human plasma or site of infection *in vitro* pharmacokinetic (PK) [5,6]. Bacteria grow in an enclosed bioreactor threaded with semi-permeable hollow fibers (i.e., a cartridge), which separate the system into two compartments: an extra-capillary space (ECS) where bacteria are harboured, and an intra-capillary space (ICS) where drugs are infused. The majority of nutrients, bacterial metabolites and compounds diffuse across the hollow fibers' pores, with different molecular weight cut-offs (MWCO), thereby equilibrating the content of both compartments. These pores are too small for bacteria to leave the ECS into the primary flow path inside the fibers, but they enable media to be constantly refreshed at a specific flow rate, as well as the addition and gradual clearance of drugs to and from the ECS [7-9]. Altogether, these traits allow users to mimic the PK profile of antimicrobial agents in the HFS-TB, and expose bacteria to a predefined posology to infer pharmacodynamic (PD) responses linked to said PK profiles. In combination with PKPD modelling and simulation, the HFS-TB may forecast clinical outcomes with a predictive accuracy of ca. 94.4% [10]. For instance, this technique can emulate dissimilar posology (e.g., once daily, QD *vs.* every other day, QAD). Further, HFS-TB readouts can unveil PKPD drivers for antibacterial activity of the unbound drug fraction, namely: area under the concentration-time curve (AUC), maximal concentration ($C_{max}$) or percentage of time (%fT), over the minimal inhibitory concentration (MIC), i.e., AUC/MIC, $C_{max}$/MIC or %fT/MIC, respectively [11-14]. In line with this, the HFS-TB can inform the design of

clinical trials including novel or repurposed anti-TB compounds [15-17], as well as drug combinations [18-20], among other possibilities. In addition, this methodology allows repetitive sample collection, is not time-limited, enables bacteria to reach high densities (similar to the ones found at the sites of infection) and lacks the ethical concerns associated with animal models, besides other advantages over alternative *in vitro* and *in vivo* preclinical tools [21].

Nonetheless, the HFS-TB is a relatively novel technology, with few research groups actively using it. This situation is, in part, due to the fact that existing literature lacks standard procedures, thorough recommendations, quality control tests and/or consolidated experimental technical guidelines [8,22], a predicament that, along with the high cost and infrastructure requisites needed to implement the HFS-TB, hinders further spreading to other laboratories, thereby curbing technology adoption [23]. One of the most relevant procedures traditionally dismissed in the field is the report of the compatibility between the drug(s) of interest and the materials throughout the system; particularly, the hollow fibers within the cartridge. The physicochemical properties of the antimicrobials (or new molecules in development) may dictate non-specific binding to said materials, and therefore they might not be able to penetrate the semi-permeable membrane and diffuse between compartments. In particular, lipophilicity could play a substantial role in this matter, since as logP increases, there is an increased probability of binding to unspecific hydrophobic targets [24,25]. Hence, the compatibility of the compounds with the constituents of the HFS-TB must be assessed prior to launching PKPD experiments to ensure proper reproduction of the desired PK profile at the ECS, where bacteria reside. In spite of its utmost relevancy, validation of the compatibility of the drug(s) under study with the HFS-TB and confirmation of achievement of the desired PK profile within the ECS are hardly addressed in works published on HFS-TB [8].

In this study, we inform on the compatibility of 10 anti-TB compounds: bedaquiline (BDQ, B), clarithromycin (CLA), delamanid (DLM), ethambutol (EMB), isoniazid (INH), linezolid (LZD, L), moxifloxacin (MXF), pretomanid (PTD, Pa), rifampicin (RMP) and rifapentine (RPT) [26,27], with the three most common hollow-fiber cartridges materials: polysulfone (PS), polyvinylidene fluoride (PVDF) and cellulose. We carried out multiple dosing to check drugs' compatibility, which yields a more complete summary of the molecules' behaviour in the HFS-TB than previously reported. Furthermore, we designed a robust strategy to simulate the PK of BDQ, PTD and LZD in combination (i.e., BPaL therapy for drug-resistant TB [28]), a challenging combination to work with in the HFS-TB due to the highly lipophilic nature of BDQ and PTD. With this information, we provide an open toolkit to ease the standardization of HFS-TB experiments and its wider implementation.

## RESULTS

**Ethambutol and linezolid fit within the compatibility range for tested HFS-TB fibers.** EMB was compatible with PS, PVDF and cellulose cartridges: the $AUC_{0\text{-}24h,\ ECS,\ ratio}$ (ca. 1.2) and the $C_{max,\ ss,\ ECS,\ ratio}$ (1.3, 0.8 and 1.2 for PS, PVDF and cellulose fibers, respectively) fit the required compatibility range. The drug was also cleared from the cartridge as expected, i.e., actual $T_{1/2}$ in the ECS met established criteria (**Figure 1a**, **Table 1**). It is worth outlining that PVDF fibers, though compatible with EMB, may not be the most suitable ones to work with this anti-TB drug since $C_{max,\ ss,\ ECS}$ was not reached until administration of the second dose (**Figure 1a**, **Table S1**).

The PK profile of LZD was also accurately simulated within the compatibility range in either type of HFS-TB cartridge, i.e., $AUC_{0\text{-}24h,\ ECS,\ ratio}$ (0.9, 0.9 and 0.8), $C_{max,\ ss,\ ECS,\ ratio}$ (1, 0.8 and 0.8) and $T_{1/2,\ ECS,\ ratio}$ (1.3, 1.4 and 1.1) for PS, PVDF and cellulose fibers,

115 respectively (**Figure 1b**, **Table 1**). Although no major differences in the AUC were
116 observed between these materials, measured $C_{max, ss, ECS}$ were closer to expected when
117 using PS fibers (**Figure 1b**, **Table S1**). Therefore, PS cartridges stood out as the most
118 adequate to perform HFS-TB assays with LZD.

119 Drug concentrations in the ECS for both drugs were slightly lower than those measured
120 in the ICS during the first samplings, indicating that a short time lapse may be needed to
121 reach equilibrium between both compartments. In contrast, these concentrations were
122 slightly higher than those detected in the ICS during days 2 and 3, thereby suggesting
123 some degree of accumulation (**Figure 1**, **Table S1**).

124 **Several anti-TB drugs fit within the compatibility range only for specific types of**
125 **HFS-TB fibers**. INH was compatible with PS and cellulose cartridges, as endorsed by
126 the observed PK parameters within the compatibility range: $AUC_{0\text{-}24h, ECS, ratio}$ (1.1 and
127 0.9), $C_{max, ss, ECS, ratio}$ (0.7 and 0.9) and $T_{1/2, ECS, ratio}$ (1.3 and 1.3) for PS and cellulose,
128 respectively. To the contrary, INH measured $AUC_{0\text{-}24h, ECS, ratio}$ and $C_{max, ss, ECS}$ in PVDF
129 cartridges did not match the criteria (0.4 and 0.4, respectively) (**Figure 2a**, **Table 2**).

130 The observed PK parameters for CLA and MXF fit compatibility requirements when
131 tested with PS fibers: $AUC_{0\text{-}24h, ECS, ratio}$ (1.1 and 1.1), $C_{max, ss, ECS, ratio}$ (0.9 and 1) and $T_{1/2,}$
132 $_{ECS, ratio}$ (1.3 and 0.9), respectively; but not with PVDF fibers, for which their calculated
133 $C_{max, ss, ECS, ratio}$ (0.5 and 0.6) and $T_{1/2, ECS, ratio}$ (3.9 and 2.6) notably differed from targeted
134 compatibility ranges for CLA and MXF, respectively, and $AUC_{0\text{-}24h, ECS, ratio}$ (0.7) for
135 MXF. Likewise, cellulose fibers were outside the compatibility range with both
136 compounds, because of divergences in $T_{1/2, ECS, ratio}$ (1.7 and 1.6 for CLA and MXF,
137 respectively). Given that the other PK traits were adequately imitated, these fibers might

still be suitable for these antimicrobial agents after proper experimental adjustments (**Figure 2b-c**, **Table 2**).

RMP was recently described not to be used with PS [22]. Similarly, the PK profile of RMP was not adequately mimicked in the HFS-TB when using PVDF cartridges (**Figure 2d** and **Table 2**). Most concentration values from the ECS were below the expected profile, indicating unspecific binding of the drug to the components of the system (**Table S1**). Thence, $AUC_{0\text{-}24h,\ ECS,\ ratio}$ and $C_{max,\ ss,\ ECS,\ ratio}$ were much lower than required: 0.4 and 0.2, respectively (**Table 2**). Moreover, $T_{1/2}$ could not be calculated because no exponential decline in RMP concentrations was registered along the time course of the experiment (**Figure 2d**). Concerning cellulose fibers, RMP's $AUC_{0\text{-}24h,\ ECS,\ ratio}$, $C_{max,\ ss,\ ECS,\ ratio}$ and $T_{1/2,\ ECS,\ ratio}$ did not meet the compatibility range requirements either; however, their values were the nearest to fit within the ranges among all tested types of fibers: 1.6 (*vs* 0.8-1.25), 0.6 (*vs* 0.7-1.3) and 2.5 (*vs* 0.6-1.4), respectively (**Table 2**). To note that the first RMP dose rendered a slightly higher $C_{max,\ ss,\ ICS}$ than expected (**Figure 2d**), which could be due to minor discrepancies between the targeted and actual syringe stock. This might have counterbalanced the decline in concentration of RMP that diffusion between ICS and ECS entailed in PVDF fibers, thus rising $C_{max,\ ss,\ ECS}$. Overall, these results indicate that, upon certain adjustments -i.e., adding extra amount of compound and/or using top-up compensation dosing-, cellulose fibers should be the ones of choice when working with RMP in the HFS-TB. In light of this knowledge and taking into account RPT's chemical resemblance with RMP [29], RPT's compatibility was only checked with cellulose fibers. As shown in **Figure 2e** and **Table 2**, $AUC_{0\text{-}24h,\ ECS,\ ratio}$ sided with the expected: 0.8 (range 0.8-1.25), while $C_{max,\ ss,\ ECS,\ ratio}$ = 0.6 (range 0.7-1.3) and $T_{1/2,\ ECS,\ ratio}$ = 1.6 (range 0.6-1.4) were near to meet compatibility requirements, supporting the use of

cellulose cartridges to work with RPT in the HFS-TB. Thence, results from these assays suggest the sole validity of cellulose to test rifamycins in the HFS-TB.

For most of these molecules, a general tendency was discerned: concentrations in the ECS were lower than those detected in the ICS, especially in the case of drug-fiber duos outside the compatibility range -e.g., RMP-PVDF-. This may indicate that a small fraction of the compounds is unable to traverse the membrane between compartments due to binding issues. Nevertheless, there were still a few cases in which a minor degree of compound accumulation in the ECS was observed during the assay, particularly during the samplings of the third dose -e.g., CLA-cellulose- (**Figure 2**, **Table S1**).

**Sub-optimal drug-fiber compatibilities might be overcome with methodological adjustments.** PTD and DLM were outside the compatibility range with all fibers (**Figure 3** and **Table 3**). Most PK parameters for PTD largely differed from the targeted compatibility ranges: $AUC_{0\text{-}24h,\ ECS,\ ratio}$ (0.3, 0.006 and 0.4), $C_{max,\ ss,\ ECS,\ ratio}$ (0.2, 0.005 and 0.2) and $T_{1/2,\ ECS,\ ratio}$ (2.5, 2.5 and 1.2) for PS, PVDF and cellulose fibers, respectively. Nearly all DLM calculated ratios of PK parameters were below the expected ones: $AUC_{0\text{-}24h,\ ECS,\ ratio}$ (0.001, 0.001 and 0.2) and $C_{max,\ ss,\ ECS,\ ratio}$ (0.002, 0.002 and 0.1) for PS, PVDF and cellulose fibers, respectively; while$T_{1/2,\ ECS,\ ratio}$ could only be calculated for cellulose fibers (0.9), since no exponential decline in DLM concentrations was discerned in the other two materials (**Figure 3a-b**, **Table 3**, **Table S1**). Altogether, these results placed PTD and DLM outside the compatibility range with all tested HFS-TB fibers. Nonetheless, it could be ascertained that cellulose fibers were the ones that gave rise to PK profiles with the highest similarity to the targeted ones. In fact, their $T_{1/2,\ ECS,\ ratio}$ entered the required range for both compounds, which suggests that the unbound drug fraction was being accurately cleared. Ergo, upon further optimization, cellulose might be the fibers of choice to work with PTD and DLM in the HFS-TB.

As a first approach, the fiber's compatibility of BDQ was tested with a non-clinical single dose with a $C_{max}$ holding step in PS and PVDF fibers, being outside the compatibility range with both fibers (**Figure 3c** and **Table 3**). $AUC_{0\text{-}24h,\ ECS,\ ratio}$ (0.002) and $C_{max,\ ss,\ ECS,\ ratio}$ (0.006) were below the compatibility range in PVDF fibers, whereas $T_{1/2,\ ECS,\ ratio}$ in this cartridge and all PK parameters in PS fibers could not be calculated, because most samplings, especially in the ECS, were below the limit of quantification of the LC-MS/MS (**Table S1**). These results posed BDQ as the most challenging compound in our compilation to work with in the HFS-TB.

In an attempt to overcome these challenges, and considering the extended terminal half-life of BDQ in the clinic [30], a modified experimental approach was designed to detect BDQ in the system and optimize its PK profile. First, the use of polypropylene and silicone materials was minimized to avoid unspecific binding [31,32]. Second, data from the compatibility tests and the TB-Platform for the Aggregation of Preclinical Experiments Data (TB-APEX) [33] were used to calculate the amount of drug and number of infusions needed to reach the targeted PK. In that sense, BDQ median concentration at protein-unbound steady state in the lung ($C_{med,\ ss}$ = 0.061 µg/mL) was aimed instead of the usual PK parameters ($AUC_{0\text{-}24h}$, $C_{max,\ ss}$ and $T_{1/2}$) [30]. Third, BDQ was directly infused in the ECS, in order to circumvent drug loss through the barrier between compartments. With this approach, the $C_{med,\ ss}$ was accurately imitated in PVDF fibers (0.082 µg/mL), unlike in PS fibers (0.008 µg/mL) and cellulose ones (0.571 µg/mL) (**Figure 4** and **Table S2**). Nevertheless, cellulose showed higher BDQ concentrations than targeted ones. This suggests that the binding that was taken into consideration to program drug infusions was overestimated in cellulose, which is in agreement with the more promising behaviour of PTD and DLM within these fibers (**Figure 3a-b**). Fluctuations in BDQ levels were registered in all fibers, but most measurements in PVDF and cellulose fit within a close

range: 0.036 to 0.090 µg/mL and 0.200 to 1.287 µg/mL, respectively. Hence, though further adjustments would be needed to refine the PK profile of BDQ in the HFS-TB, this approach could help to pave the way towards the use of lipophilic compounds in the HFS-TB.

**Pharmacokinetic profile mimicking of the BPaL combination in the HFS-TB.** We took advantage of our assay toolkit for anti-TB drugs in the HFS-TB to design an optimal setup for BPaL testing. As a proof-of-concept, we targeted a 3-days PK profile of BDQ, PTD and LZD in a cellulose cartridge, based on our previously generated monotherapy data. An unbound $C_{med,\ ss}$ in the lung was aimed for BDQ, whilst PTD's PK profile was targeted by infusing higher amounts of drug and top-up compensations, in order to overcome unspecific binding and countervail LZD's clearance rate, respectively.

As displayed in **Figure 5**, $C_{med,\ ss}$ of BDQ was correctly reproduced: 0.050 µg/mL (*vs* 0.061 µg/mL), and most measurements fit within a small range: 0.014 to 0.099 µg/mL (**Table S3**). Likewise, LZD's PK parameters fit compatibility requirements: $AUC_{0\text{-}24h,\ ECS,\ ratio}$ = 1.2 (0.8-1.25), $C_{max,\ ss,\ ECS,\ ratio}$ = 0.8 (0.7-1.3) and $T_{1/2,\ ECS,\ ratio}$ = 1.2 (0.6-1.4) (**Table 1**). Conversely, PTD's $T_{1/2,\ ECS,\ ratio}$ sided with the expected (0.8 *vs* 0.6-1.4), but $AUC_{0\text{-}24h,\ ECS,\ ratio}$ = 0.5 (*vs* 0.8-1.25) and $C_{max,\ ss,\ ECS,\ ratio}$ = 0.4 (*vs* 0.7-1.3) were outside the compatibility range. However, these values were near our requirements and notably improved the results from PTD's compatibility test alone (**Table 3**). Given that $T_{1/2,\ ECS}$ was accurately mimicked, $AUC_{0\text{-}24h,\ ECS}$ and $C_{max,\ ss,\ ECS}$ could be easily boosted by increasing PTD's concentration in each infusion.

## DISCUSSION

The HFS-TB has become a useful *in vitro* preclinical tool to characterize PKPD profiles of new and repurposed antibiotics and regimens for TB treatment, as well as informing

the design of prospective clinical trials [6]. However, access to essential information needed for inter-laboratory experimental reproduction of results has been elusive. Indeed, recent publications in the field have emphasized the urgent need for standard procedures and experimental specifications in HFS-TB reports, to facilitate laboratories to *de novo* implement this technology [8,22,34]. Delivering this information will increase capacity and provide confidence in published data, allowing researchers to reproduce them.

The lack of information on the compatibility between drugs and the different types of hollow fibers stands out as a major limitation in the use of the HFS-TB. In this sense, it is relevant to stress that not all molecules are compatible with the materials the cartridges are made of: they may bind to the hollow fibers, plastics or other components of the system; and/or they may not be able to penetrate the semi-permeable membrane of said fibers. Therefore, as advised by Aguilar-Ayala *et al.* [22], compatibility tests for the drug(s) of interest in the absence of bacteria should be routinely assessed and reported prior to conducting PKPD experiments in the HFS-TB. To shorten this gap, in this work, we carried out compatibility tests with the three most common hollow-fiber materials, i.e., PS, PVDF and cellulose, and a catalogue of 10 drugs including representatives of distinct anti-TB families, so as to span a wide window of chemical features: ethanolamines (EMB), diarylquinolines (BDQ), INH, macrolides (CLA), nitroimidazoles (PTD, DLM), oxazolidinones (LZD), quinolones (MXF) and rifamycins (RMP, RPT) (**Figure 6**). Further, a currently prominent three-drug combination in the anti-TB field (BPaL, featuring BDQ, PTD and LZD) was assayed in the system upon the information gathered from the drug-fiber compatibility tests of each antibiotic alone. A specific PK profile of each antimicrobial was targeted in the system in absence of bacteria, and its accuracy was verified by measuring drug levels in the ICS and ECS over time. Compatibility ranges were established based on obtained $AUC_{0\text{-}24h,\ ECS}$, $C_{max,\ ss,\ ECS}$ and $T_{1/2,\ ECS}$ compared to

the expected parameters [35]. It is of note that drug concentrations in the ECS have been scarcely reported in the field, despite being the compartment where bacteria actually face the compound(s) and the actual pharmacodynamic interaction occurs.

Our results indicate the following: (i) EMB and LZD fit within the compatibility range with the three types of fibers; (ii) INH with PS and cellulose, but not with PVDF; (iii) CLA and MXF only with PS; (iv) rifamycins (RMP, RPT) could only be used with cellulose; (v) PTD and DLM were outside the compatibility range with all fibers, but their PK profiles in cellulose cartridges appeared more promising upon further modifications; (vi) BDQ was outside the compatibility range with PS and PVDF fibers, but alternative approaches could be implemented to overcome this issue (**Figures 1-4** and **6**, **Tables 1-3**). These results accentuate the importance of deciphering the suitability of each compound with the HFS-TB cartridges before performing PKPD studies, as many of them were unfit to be used with at least some of the fibers' materials. We could also infer that PVDF cartridges are the least user-friendly, since they were outside the compatibility range with 7 out of 9 compounds (BDQ, CLA, DLM, INH, MXF, PTD and RMP). PS fibers were the most suitable for 5 out of 9 compounds tested (CLA, EMB, INH, LZD and MXF). In contrast, cellulose cartridges seem to be the most versatile ones; although only 3 out of 10 compounds were within the compatibility range, they would allow working with of all the compounds in our panel -upon infusions' adjustments- with different degrees of lipophilicity (**Figure 6**).

HFS-TB studies have traditionally only reported drug levels at the ICS, thereby disregarding the ECS, where bacteria are effectively exposed to the drug [34,36,37]. This work, along with Aguilar-Ayala *et al.* [22], reinforces the fact that there are usually non-negligible discrepancies between the drug concentrations in the ICS and the lumen of the cartridges (i.e., ECS), being the latter the one that should be rigorously reported. These

permeability issues might be due to the pore's and fiber's inner diameter, the membrane surface area or the effective length of the tubing, among other factors related to the system itself [38]; but also to the hydrophilicity/lipophilicity attributes of the compounds and the components of the system.

Regarding this hydrophilicity/lipophilicity dichotomy, the general tendency we observed is that molecules with the lowest logP and highest water solubility showed less binding to the fibers and free diffusion between the ICS and the ECS (**Figure 6**). This applied to EMB and LZD, with low experimental and/or predicted logP (0.4 and 0.9 for EMB and LZD, respectively), which is usually associated with low lipophilicity [39]. Their water solubility is high as well: 1,000 mg/mL and 3 mg/mL, respectively (**Table S4**). INH also shows high hydrophilicity (logP = -0.7) and water solubility (140 mg/mL), but did not fit within the compatibility range with PVDF fibers. This is likely because the concentrations quantified in the first samplings were below the expected ones, thus rendering an overall $AUC_{0\text{-}24h,\ ECS,\ ratio}$ and $C_{max,\ ss,\ ECS,\ ratio}$ that deviated from the required criteria (**Figure 2a**, **Table 2**). By adjusting the amount of INH in the first dosing to compensate for this delay in the equilibrium between compartments, the INH-PVDF drug-fiber duo might be turned into a compatible pair for HFS-TB experiments. Nonetheless, only INH-PS or INH-cellulose duos have been published to date [40,41], so this hypothesis should be further confirmed. In contrast, drugs with medium-high lipophilicity (e.g., PTD and DLM: predicted logP = 4.14 and 6.14 and water solubility = -<1 mg/mL and 0.0022 mg/mL, respectively; **Table S4**) did not meet the compatibility ranges for most PK parameters and hardly passed through the fibers' membrane, probably due to unspecific binding. Interestingly, they were prone to behave better in cellulose (or PS, in the case of PTD) than in PVDF, for which a sizable degree of binding was ascertained (**Figure 3**, **Table 3**, **Table S1**). This may be justified by the lipophilicity of the fibers themselves: PVDF

311 appears to be the most hydrophobic, whereas cellulose would be the most hydrophilic,
312 followed by PS [42,43]. As a consequence, it is not unforeseen that cellulose worked better
313 with BDQ, DLM, PTD, RMP or RPT (which are among those with the highest logP)
314 because a hydrophilic ambience may prevent hydrophobic compounds from sticking to
315 inner surfaces [44]. In brief, our work supports these observations and suggest that
316 deepening into the chemical properties -mainly logP and water solubility- of the drug(s)
317 under study prior to performing HFS-TB assays could aid the selection of the most
318 accurate cartridge to work with. Nevertheless, cellulose fibers outstand as the most
319 versatile choice when dealing with highly lipophilic molecules.

320 It is worth highlighting that some PK parameters of RMP, RPT and, specially, BDQ,
321 DLM and PTD were not successfully mimicked in any of the cartridges tested (**Tables 2-**
322 **3**), which according to our criteria placed them outside the compatibility range. In fact,
323 as depicted in **Figure 3**, a sizable amount of compound was lost when crossing the semi-
324 permeable hindrance between the ICS and the ECS. Several strategies could be adopted
325 to overcome this hurdle, as the ones we applied to BDQ: (i) rising the amount of
326 compound in each infusion, (ii) using compensating infusions to keep a median
327 physiological concentration and (iii) adding the drug directly into the ECS to avoid the
328 barrier between compartments. In addition, hydrophilicity performance of the fibers can
329 be enhanced, which might reduce the unspecific binding of hydrophobic molecules. This
330 has been previously addressed with PS hollow-fiber membranes, using calcium alginate,
331 zinc oxide or graft polymerization with 2-hydroxyethylacrylate, among other possibilities
332 [45-48]; albeit, extrapolation to hollow-fiber cartridges would require further research.
333 Oppositely, a hydrophobic coating may saturate the unspecific binding sites of the HFS-
334 TB materials and, as a consequence, prevent drug levels to decline. This strategy was
335 employed by Raaijmakers J. *et al* [31] using clofazimine to block the binding sites of BDQ.

However, this alternative was ruled out in this study since clofazimine has antibacterial activity against *M. tuberculosis* [49].

In this work, we propose criteria to decide whether a drug is within the compatibility range or not with a certain type of hollow-fiber cartridge, based on three primary PK parameters in the ECS ($AUC_{0\text{-}24\ h}$, $C_{max,\ ss}$ and $T_{1/2}$). This classification lies within a methodological perspective that aims to inform on the most suitable cartridges when working with certain compounds in the system. Albeit, it should be remarked that HFS-TB experiments are often used to feed *in silico* models to inform the design of clinical trials [10]. This means that modelling might still benefit from data derived from a duo outside the compatibility range, e.g., INH-PVDF, CLA-Cellulose or MXF-Cellulose. Many drugs included in this study had AUC/MIC as their PKPD driver for antibacterial efficacy [50-53], being thus $AUC_{0\text{-}24h,\ ECS,\ ratio}$ a credible parameter to validate their PK; however, murine models have described PTD activity as time-dependent and its bactericidal activity best associated with the percentage of the dosing interval in which free drug concentration surpasses the MIC (%fT/MIC) [54]. Being 0.125-0.25 µg/mL the MIC to PTD of *M. tuberculosis* H37Rv strain [55], we were able to kept a 100% fT/MIC to PTD in our compatibility tests with PS and cellulose fibers. This indicates that, depending on the research goal, PTD may be used in the HFS-TB to provide useful PKPD outputs despite the technical quandary this drug entails. As a final note, we ought to state that preliminary compatibility tests do not replace the need to report further PK measurements during actual HFS-TB PKPD experiments with bacteria [56].

BPaL therapy has dramatically changed the management of drug resistant TB [28]. However, to our knowledge, only a few publications have reported BPaL results in the HFS-TB [16,20]. In fact, an accurate reproduction of its combined PK profile poses a significant challenge, due to the highly lipophilic nature of BDQ and PTD. By leveraging

on our drug-fiber compatibility studies, we obtained information on their behavior within each cartridge, defined adjustments to refine their PK profiles and developed a robust strategy to simulate a combined PK profile of BDQ, PTD and LZD (**Figure 4**). In spite of PTD not fitting the compatibility range for 2 out of 3 PK parameters (**Table 3**), our results proved the importance of previous drug-alone tests, being accurate enough to facilitate the implementation of this combination in the HFS-TB. Since BPaL is one of the most important TB treatments against drug-resistant TB, and with the emerging concern of BDQ-resistant strains presenting mutations in the *rv0678c* gene [57], the methodological improvements here reported hold major significance to aid in the optimization of the treatment against BDQ-resistant strains.

In summary, in this work we provide a comprehensive analysis of the suitability of the most common hollow-fiber materials to be used in the HFS-TB with anti-TB drugs to date. Our data show that several types of fibers are not suitable to work with certain compounds, and that measuring the actual drug concentrations that bacteria face inside the ECS (which are usually lower than expected) is crucial, underpinning that drugs should be tested for compatibility with the HFS-TB before carrying out a PKPD assay, either in monotherapy or combinations. We also provide a theoretical rationale to pre-select the cartridge material to be used for each new drug, which is based on a relationship between the hydrophilicity/lipophilicity of the molecules and the compatibility with fibers' materials. We hope that this report is of use to other laboratories trying to implement and optimize HFS-TB PKPD experiments. We also encourage other laboratories working with the HFS-TB to readily disclose this type of information for additional compounds not here tested. This collaborative framework would make a noteworthy step towards reaching best-practice principles that this preclinical technique should own to maximize its role in informing the design of Phase II/III clinical trials.

## RESOURCE AVAILABILITY

### Lead contact

Requests for further information and resources should be directed to and will be fulfilled by the lead contact, Fernando Sanz-García (f.sanzg@unizar.es).

### Materials availability

This study did not generate new unique reagents.

### Data and code availability

• Data reported in this paper will be shared by the lead contact upon request.

• This paper does not report original code.

• Any additional information required to reanalyze the data reported in this paper is available from the lead contact upon request.

### Limitations of the study

Our compatibility results were mostly based on PK profiles in the lung, which were derived from specific dosing chosen among the most commonly used for each antibiotic. However, depending on the research question, special situations and patient populations -e.g., children- might require alternative dosing strategies or mimicking PK profiles in different compartments -e.g., plasma *vs.* lung-. If these differences entailed major changes in expected drug concentrations, the compatibility of the molecule with the HFS-TB fibers might differ, assuming its binding is concentration-dependent. Thus, we advise users to ensure desired PK profiles are properly mimicked in their experimental setup.

Although PS, PVDF and cellulose are by far the main fibers' materials used in the HFS-TB field, other options could have been examined to expand our assay toolkit, -e.g., polyethersulfone cartridges [58]-, especially when facing highly lipophilic compounds.

Similarly, we have limited our study to some representative anti-TB drugs; other less commonly used or currently under development were not included in our study because of lack of access to the compound or capacity limitations. However, we hope that, by assaying this initial "toolkit", we contribute to the creation of a working framework that could enhance essential data accessibility to robustly performed HFS-TB studies. Additional contributions from the field would enlarge this assay toolkit for HFS-TB with more antibiotics.

## ACKNOWLEDGEMENTS

We would like to thank the technical support of Ana Picó Marco from the University of Zaragoza, and the recommendations on targeted PK parameters for BPaL combination of Evangelos Karakitsios, from Institute for Applied Computing "Mauro Picone", Consiglio Nazionale delle Ricerche.

This work has received support from the Innovative Medicines Initiatives 2 Joint Undertaking (grant No 853989) to NW and SRG. The JU receives support from the European Union's Horizon 2020 Research and Innovation Programme and EFPIA and Global Alliance for TB Drug Development Non-Profit Organisation, Bill & Melinda Gates Foundation, University of Dundee.

## AUTHOR'S CONTRIBUTIONS

CRediT (Contributor Roles Taxonomy) has been applied for author contribution.

Conceptualization: FSG, AL, SRG; Data curation: FSG; Formal Analysis: FSG, MREM DN; Funding acquisition: NW, SRG; Investigation: FSG, DAAA, MREM, DN, AB, SA, NI; Methodology: FSG, DAAA, AML, AL, SRG; Project administration: NW, AL, SRG; Supervision: NW, AL, SRG; Visualization: FSG, DAAA; Writing – original draft: FSG,

AL, SRG; Writing – review & editing: FSG, DAAA, MREM, DN, AL, SRG. All authors read and approved the final version of the document.

## DECLARATION OF INTERESTS

The authors declare no competing interests.

**Figure 1 | Drug-fiber compatibility tests of ethambutol and linezolid in the HFS-TB.** Expected (dashed line) and observed (solid lines) pharmacokinetic (PK) profiles of **(a)** ethambutol and **(b)** linezolid, sampled from the intra-capillary space (ICS; green line) and extra-capillary space (ECS; purple line) of polysulfone (PS), polyvinylidene fluoride (PVDF) and cellulose HFS-TB cartridges. Targeted PK parameters for each antibiotic are described in **Table 4**. Drug concentration values are provided in **Table S1**. EMB: ethambutol, LZD: linezolid.

**Figure 2 | Drug-fiber compatibility tests of isoniazid, clarithromycin, moxifloxacin, rifampicin and rifapentine in the HFS-TB.** Expected (dashed line) and observed (solid lines) pharmacokinetic (PK) profiles of **(a)** isoniazid, **(b)** clarithromycin, **(c)** moxifloxacin, **(d)** rifampicin and **(e)** rifapentine, sampled from the intra-capillary space (ICS; green line) and extra-capillary space (ECS; purple line) of polysulfone (PS), polyvinylidene fluoride (PVDF) and cellulose HFS-TB cartridges. Targeted PK parameters for each antibiotic are described in **Table 4**. Drug concentration values are provided in **Table S1**. CLA: clarithromycin; INH: isoniazid; MXF: moxifloxacin; RMP: rifampicin; RPT: rifapentine.

**Figure 3 | Drug-fiber compatibility tests of pretomanid, delamanid and bedaquiline in the HFS-TB.** Expected (dashed line) and observed (solid lines) pharmacokinetic (PK) profiles of **(a)** pretomanid, **(b)** delamanid and **(c)** bedaquiline, sampled from the intra-capillary space (ICS; green line) and extra-capillary space (ECS; purple line) of polysulfone (PS), polyvinylidene fluoride (PVDF) and cellulose HFS-TB cartridges. Targeted PK parameters for each antibiotic are described in **Table 4**. Drug concentration values are provided in **Table S1**. BDQ: bedaquiline; DLM: delamanid; PTD: pretomanid.

**Figure 4 | Optimization approach to use bedaquiline in the HFS-TB.** Observed pharmacokinetic (PK) profiles of bedaquiline, sampled from the extra-capillary space

(ECS) of polysulfone (PS), polyvinylidene fluoride (PVDF) and cellulose HFS-TB cartridges. The targeted median concentration at protein-unbound steady state in the lung ($C_{med, ss}$ = 0.061 µg/mL) is indicated in **Table 4** and represented in the graphs by a dashed line. Drug concentration values are provided in **Table S2**. BDQ: bedaquiline.

**Figure 5 | Optimization approach to use bedaquiline-pretomanid-linezolid (BPaL) combination in the HFS-TB.** Expected (dashed lines) and observed (solid purple lines) pharmacokinetic (PK) profiles of a combination of bedaquiline, pretomanid and linezolid (i.e., BPaL) sampled from the extra-capillary space (ECS) of a cellulose HFS-TB cartridge. The targeted median concentration at protein-unbound steady state in the lung of BDQ ($C_{med, ss}$ = 0.061 µg/mL) is indicated in **Table 4** and represented in the graph by a straight dashed line. Likewise, targeted PK parameters for pretomanid and linezolid are described in **Table 4.** Drug concentration values are provided in **Table S3**. BDQ: bedaquiline, PTD: pretomanid, LZD: linezolid.

**Figure 6 | Schematic drug-fiber compatibility status of anti-TB drugs in the HFS-TB.** Anti-TB drugs are ordered based on their lipophilicity. Experimental and predicted logP values are encompassed in **Table S4**. PS: polysulfone; ND: not determined; BDQ: bedaquiline; CLA: clarithromycin; DLM: delamanid; EMB: ethambutol; INH: isoniazid; LZD: linezolid; MXF: moxifloxacin; PTD: pretomanid; RMP: rifampicin; RPT: rifapentine.

*Optimization approach showed in **Figure 4** rendered cellulose as the fibers with less binding to BDQ.

## STAR★METHODS

- **Key resources table**
- **Method details**
  - Culture media and drugs
  - HFS experimental set up
  - Mimicking a pharmacokinetic profile in the HFS for drug-fiber compatibility tests
  - Optimization approach to mimic a pharmacokinetic profile of bedaquiline in the HFS-TB
  - Optimization approach to mimic a pharmacokinetic profile of bedaquiline-pretomanid-linezolid (BPaL) combination in the HFS-TB
  - Preparation of drug samples and drug quantification
- **Quantification and statistical analysis**

## SUPPLEMENTAL INFORMATION

**Document S1.** Figure S1, Tables S2-S6 and supplemental references.

**Table S1.**

**Table 1. Comparison of pharmacokinetic parameters of different drugs within the compatibility range for three types of HFS-TB fibers.**

| Drug | Expected PK parameters | | | PS | | | | | | PVDF | | | | | | Cellulose | | | | | |
|---|---|---|---|---|---|---|---|---|---|---|---|---|---|---|---|---|---|---|---|---|---|
| | $AUC_{0\text{-}24h}$ (µg*h/mL) | $C_{max,\ ss}$ (µg/mL) | $T_{1/2}$ (h) | $AUC_{0\text{-}24h}$ (µg*h/mL) (ratio) | | $C_{max,\ ss}$ (µg/mL) (ratio) | | $T_{1/2}$ (h) (ratio) | | $AUC_{0\text{-}24h}$ (µg*h/mL) (ratio) | | $C_{max,\ ss}$ (µg/mL) (ratio) | | $T_{1/2}$ (h) (ratio) | | $AUC_{0\text{-}24h}$ (µg*h/mL) (ratio) | | $C_{max,\ ss}$ (µg/mL) (ratio) | | $T_{1/2}$ (h) (ratio) | |
| | | | | ICS | ECS | ICS | ECS | ICS | ECS | ICS | ECS | ICS | ECS | ICS | ECS | ICS | ECS | ICS | ECS | ICS | ECS |
| EMB | 24 | 3 | 3[a] | 32 (1.2) | 31 (1.2) | 4 (1.3) | 4 (1.3) | 3.3 (1.1) | 3.6 (1.2) | 22.5 (0.9) | 29.6 (1.2) | 3.1 (1) | 2.5 (0.8) | 3.4 (1.1) | 3.9 (1.3) | 25 (1.0) | 28.8 (1.2) | 3.7 (1.2) | 3.6 (1.2) | 3.3 (1.1) | 4.1 (1.4) |
| | | | 12[a] | | | | | 13.9 (1.2) | 8.7 (0.7) | | | | | 9.2 (0.8) | 9 (0.8) | | | | | 10.5 (0.9) | 9 (0.8) |
| LZD (alone) | 57.8 | 8.6 | 3.5 | 55.3 (0.9) | 54.7 (0.9) | 8.5 (1) | 8.6 (1) | 4.6 (1.3) | 4.7 (1.3) | 53.9 (0.9) | 52.8 (0.9) | 7.6 (0.9) | 6.6 (0.8) | 5 (1.4) | 4.9 (1.4) | 52 (0.9) | 46.2 (0.8) | 8.5 (1) | 6.7 (0.8) | 4 (1.1) | 3.8 (1.1) |
| LZD (BPaL) | | | | NA | NA | NA | NA | NA | NA | NA | NA | NA | NA | NA | NA | NA | 13.7[b] (1.2) | NA | 1.3[b] (0.8) | NA | 4.5 (1.2) |

EMB: ethambutol, LZD: linezolid, BPaL: bedaquiline-pretomanid-linezolid. PS: polysulfone, PVDF: polyvinylidene fluoride, SS: steady state, ICS: intra-capillary space, ECS: extra-capillary space. AUC ratio is calculated as $AUC_{0\text{-}24h,\ real}/AUC_{0\text{-}24h,\ expected}$. $C_{max,\ ss}$ ratio is calculated as $C_{max,\ ss,\ real}/\ C_{max,\ ss,\ expected}$, being $C_{max,ss,\ real}$ an average of the three $C_{max}$ reached during the dosing. $T_{1/2}$ ratio is calculated as $T_{max,\ 1/2,\ real}/\ T_{1/2\ expected}$, being

$T_{max,\ 1/2,\ real}$ an average of the three $T_{1/2}$ calculated for each clearance after dosing. Drug concentration values are provided in **Table S1** for drugs alone and **Table S3** for LZD in the BPaL combination.

[a]EMB's PK is best described by a two-compartment model: $T_{1/2,\alpha,\ 0\text{-}12\ h}$ = 3 h and $T_{1/2,\beta,\ 12\text{-}24\ h}$ = 12 h.

[b]Due to changes detected in the syringe stock, LZD's expected PK parameters in BPaL were re-calculated as: $AUC_{0\text{-}24h}$ = 11 µg*h/mL and $C_{max,ss}$ = 1.6 µg/mL.

528 **Table 2. Comparison of pharmacokinetic parameters of different drugs within the compatibility range with specific types of HFS-TB**

529 **fibers.**

| Drug | Expected PK parameters | | | PS | | | | | | PVDF | | | | | | Cellulose | | | | | |
|---|---|---|---|---|---|---|---|---|---|---|---|---|---|---|---|---|---|---|---|---|---|
| | $AUC_{0\text{-}24h}$ (μg*h/mL) | $C_{max,\ ss}$ (μg/mL) | $T_{1/2}$ (h) | $AUC_{0\text{-}24h}$ (μg*h/mL) (ratio) | | $C_{max,\ ss}$ (μg/mL) (ratio) | | $T_{1/2}$ (h) (ratio) | | $AUC_{0\text{-}24h}$ (μg*h/mL) (ratio) | | $C_{max,\ ss}$ (μg/mL) (ratio) | | $T_{1/2}$ (h) (ratio) | | $AUC_{0\text{-}24h}$ (μg*h/mL) (ratio) | | $C_{max,\ ss}$ (μg/mL) (ratio) | | $T_{1/2}$ (h) (ratio) | |
| | | | | ICS | ECS | ICS | ECS | ICS | ECS | ICS | ECS | ICS | ECS | ICS | ECS | ICS | ECS | ICS | ECS | ICS | ECS | ICS | ECS |
| CLA | 30.7 | 3.5 | 4 | 37.1 (1.2) | 34.3 (1.1) | 3.5 (1) | 3.1 (0.9) | 5.1 (1.3) | 5.4 (1.3) | 26.6 (0.8) | 27.3 (0.9) | 2.7 (0.8) | 1.6 (0.5) | 5.8 (1.5) | 15.5 (3.9) | 33.7 (1.1) | 35.9 (1.2) | 3.5 (1) | 2.8 (0.8) | 4.7 (1.2) | 6.9 (1.7) |
| INH | 39.6 | 6.8 | 3 | 43.6 (1.1) | 42.6 (1.1) | 6.8 (1) | 4.8 (0.7) | 4.2 (1.4) | 3.9 (1.3) | 23.7 (0.6) | 17.4 (0.4) | 5.6 (0.8) | 2.7 (0.4) | 3.5 (1.2) | 3.3 (1.1) | 34.9 (0.8) | 38.2 (0.9) | 5.5 (0.8) | 5.8 (0.9) | 3.3 (1.1) | 3.8 (1.3) |
| MXF | 45.4 | 3.1 | 13 | 50 (1.1) | 49.9 (1.1) | 3.3 (1.1) | 3.2 (1) | 12 (0.9) | 11.5 (0.9) | 36.2 (0.8) | 32.5 (0.7) | 2.4 (0.8) | 1.8 (0.6) | 32.6 (2.5) | 33.7 (2.6) | 42.1 (0.9) | 41.3 (0.9) | 2.8 (0.9) | 2.3 (0.7) | 18.7 (1.4) | 20.4 (1.6) |
| RMP | 12.5 | 2.05 | 2.5 | NA | NA | NA | NA | NA | NA | 7.6 (0.6) | 5 (0.4) | 1.3 (0.6) | 0.5 (0.2) | 4.6 (1.8) | -[a] | 22.5 (1.8) | 19.8 (1.6) | 2.7 (1.3) | 1.2 (0.6) | 3.6 (1.4) | 6.3 (2.5) |
| RPT | 12.5 | 2 | 2.5 | NA | NA | NA | NA | NA | NA | NA | NA | NA | NA | NA | NA | 10 (0.9) | 9.7 (0.8) | 1.6 (0.8) | 1.2 (0.6) | 3.2 (1.3) | 4 (1.6) |

530

CLA: clarithromycin, INH: isoniazid, MXF: moxifloxacin, RMP: rifampicin, RPT: rifapentine, BPaL: bedaquiline-pretomanid-linezolid. PS: polysulfone, PVDF: polyvinylidene fluoride, SS: steady state, ICS: intra-capillary space, ECS: extra-capillary space, NA: not applicable. AUC ratio is calculated as $AUC_{0\text{-}24h,\ real}/AUC_{0\text{-}24h,\ expected}$. $C_{max,\ ss}$ ratio is calculated as $C_{max,\ ss,\ real}/\ C_{max,\ ss,\ expected}$, being $C_{max,ss,\ real}$ an average of the three $C_{max}$ reached during the dosing. $T_{1/2}$ ratio is calculated as $T_{max,\ 1/2,\ real}/\ T_{1/2\ expected}$, being $T_{max,\ 1/2,\ real}$ an average of the three $T_{1/2}$ calculated for each clearance after dosing. Drug concentration values are provided in **Table S1**.

[a] $T_{1/2}$ could not be calculated because the actual PK profile did not follow the expected exponential decline.

538 **Table 3. Comparison of pharmacokinetic parameters of drugs outside the compatibility range with tested HFS-TB fibers.**

| Drug | Expected PK parameters | | | PS | | | | | | PVDF | | | | | | Cellulose | | | | | |
|---|---|---|---|---|---|---|---|---|---|---|---|---|---|---|---|---|---|---|---|---|---|
| | $AUC_{0\text{-}24h}$ (µg*h/mL) | $C_{max,\ ss}$ (µg/mL) | $T_{1/2}$ (h) | $AUC_{0\text{-}24h}$ (µg*h/mL) (ratio) | | $C_{max,\ ss}$ (µg/mL) (ratio) | | $T_{1/2}$ (h) (ratio) | | $AUC_{0\text{-}24h}$ (µg*h/mL) (ratio) | | $C_{max,\ ss}$ (µg/mL) (ratio) | | $T_{1/2}$ (h) (ratio) | | $AUC_{0\text{-}24h}$ (µg*h/mL) (ratio) | | $C_{max,\ ss}$ (µg/mL) (ratio) | | $T_{1/2}$ (h) (ratio) | |
| | | | | ICS | ECS | ICS | ECS | ICS | ECS | ICS | ECS | ICS | ECS | ICS | ECS | ICS | ECS | ICS | ECS | ICS | ECS |
| BDQ | 8.9 | 0.5 | 17.8 | -[a] | -[a] | -[a] | -[a] | -[b] | -[a] | 0.3 (0.03) | 0.02 (0.002) | 0.06 (0.1) | 0.003 (0.006) | 8.1 (0.4) | -[b] | NA | NA | NA | NA | NA | NA |
| DLM | 7.9 | 0.5 | 30 | 0.2 (0.02) | 0.01 (0.001) | 0.02 (0.04) | 0.0009 (0.002) | -[b] | -[b] | 0.6 (0.08) | 0.01 (0.001) | 0.08 (0.2) | 0.001 (0.002) | -[b] | -[b] | 5.7 (0.7) | 1.7 (0.2) | 0.3 (0.6) | 0.05 (0.1) | 20.4 (0.7) | 26.5 (0.9) |
| PTD (alone) | 32.7 | 2 | 18 | 21.2[c] (0.5) | 11.3[c] (0.3) | 1[c] (0.5) | 0.4[c] (0.2) | 39.7 (2.2) | 44.5 (2.5) | 1.4 (0.04) | 0.2 (0.006) | 0.2 (0.1) | 0.01 (0.005) | 16.3 (0.9) | 45.4 (2.5) | 27.6[c] (0.5) | 15.9[c] (0.3) | 1.7[c] (0.9) | 0.7[c] (0.2) | 20.7 (1.2) | 21.9 (1.2) |
| PTD (BPaL) | 70.5 | 4.3 | | NA | NA | NA | NA | NA | NA | NA | NA | NA | NA | NA | NA | NA | 30.3 (0.4) | NA | 2.2 (0.5) | NA | 15 (0.8) |

539

540 BDQ: bedaquiline, DLM: delamanid, PTD: pretomanid, BPaL: bedaquiline-pretomanid-linezolid. PS: polysulfone, PVDF: polyvinylidene fluoride,

541 SS: steady state, ICS: intra-capillary space, ECS: extra-capillary space, NA: not applicable. AUC ratio is calculated as $AUC_{0\text{-}24h,\ real}/AUC_{0\text{-}24h,}$

542 $_{expected}$. $C_{max,\ ss}$ ratio is calculated as $C_{max,\ ss,\ real}/\ C_{max,\ ss,\ expected}$, being $C_{max,ss,\ real}$ an average of the three (PTD) and two (DLM) $C_{max}$ reached during

543 the dosing, or the five samplings taken during the $C_{max}$ holding step (BDQ). $T_{1/2}$ ratio is calculated as $T_{max,\ 1/2,\ real}$/ $T_{1/2\ expected}$, being $T_{max,\ 1/2,\ real}$ an
544 average of the three (PTD), two (DLM) or one (BDQ) $T_{1/2}$ calculated for each clearance after dosing. Drug concentration values are provided in
545 **Table S1** for drugs alone and **Table S3** for PTD in the BPaL combination.

546 [a]PK parameters could not be calculated because drug concentrations were below the limit of quantification

547 [b]$T_{1/2}$ could not be calculated because the actual PK profile did not follow the expected exponential decline.

548 [c]Due to changes detected in the syringe stocks, PTD-PS and PTD-cellulose compatibility test's expected PK parameters were re-calculated as:
549 $AUC_{0\text{-}24h}$ = 40.6 µg*h/mL, $C_{max,ss}$ = 2.5 µg/mL; and $AUC_{0\text{-}24h}$ = 53.2 µg*h/mL, $C_{max,ss}$ = 3.1 µg/mL; respectively.

550

551 **Table 4. Summary of pharmacokinetic parameters for drug-fibers compatibility tests in the HFS-TB.**

| Drug | Mimicking dosing | $C_{max, ss}$ (μg/mL) | $T_{max}$ (h) | $T_{1/2}$ (h) | Total/free fraction | Site of infection | Reference |
|---|---|---|---|---|---|---|---|
| BDQ | NA | 0.5 | 1 | 17.8 | NA | NA | NA |
| | 200 mg TIW (3 days) | $C_{med, ss}$ = 0.061 μg/mL | | | Free | Lung (ELF) | Raaijmaakers et al. [31], van Heeswijk et al. [59], Alghamdi et al. [60], Moodliar et al. [61], Svensson et al. [62], Stephens et al. [63], Ngwalero et al. [64] |
| CLA | 500 mg BID (3 days) | 3.5 | 2 | 4 | Free | Plasma | Guay et al. [65] |
| DLM | 10 mg/kg QAD (4 days) | 0.5 | 3.4 | 30 | Free | Plasma | Ramirez et al. [66], TB-APEX [33] |
| EMB | 25 mg/kg QD (3 days) | 3 | 2 | 3; 12[a] | Free | Lung (ELF) | Bekker et al. [67], Tikiso et al. [68], Lee et al. [69], Srivastava et al. [70] |
| INH | 600 mg QD (3 days) | 6.8 | 1 | 3 | Free | Lung (ELF) | Gumbo et al. [20] |
| LZD | 600 mg QD (3 days) | 8.6 | 1 | 3.5 | Free | Lung (lesion) | Heinrichs et al. [14] |
| MXF | 400 mg QD (3 days) | 3.1 | 1.5 | 13 | Total | Plasma | Ginsburg et al. [71], Kim et al. [72] |
| PTD (alone) | 200 mg QD (3 days) | 2 | 1 | 18 | Free | Plasma | Lyons et al. [73], Liu et al. [74], Gumbo et al. [20] |
| PTD (BPaL) | 200 mg QD (3 days) | 4.3 | 1 | 18 | Free | Lung (lesion) | Lyons et al. [73], Liu et al. [74], Mehta et al. [75], Karakitsios et al. [76], Mehta et al. [77] |
| RMP | 600 mg QD (3 days) | 9 | 2 | 2.5 | Free | Lung (ELF) | Drusano et al. [36], Stott et al. [78] |

| | | | | | | | |
|---|---|---|---|---|---|---|---|
| RPT | 600 mg QD (3 days) | 2.05 | 2 | 2.5 | Free | Lung (ELF) | Clewe et al. [79], Stott et al. [78] |

552

553 BDQ: bedaquiline, CLA: clarithromycin, DLM: delamanid, EMB: ethambutol, INH: isoniazid, LZD: linezolid, MXF: moxifloxacin, PTD:
554 pretomanid, RMP: rifampicin, RPT: rifapentine, BPaL: bedaquiline-pretomanid-linezolid. $C_{med,\ ss}$: median concentration at protein-unbound steady
555 state in the lung, TIW: three times a week; BID: *bis in die*: twice a day; QAD: *quaque altera die*: every other day; QD: *quaque die*: once a day.
556 ELF: epithelial lining fluid. NA: not applicable.

557 [a]EMB's PK is best described by a two-compartment model: $T_{1/2,\alpha,\ 0\text{-}12\ h}$ = 3 h and $T_{1/2,\beta,\ 12\text{-}24\ h}$ = 12 h.

558

## REFERENCES


1. Gumbo, T., Louie, A., Deziel, M.R., Parsons, L.M., Salfinger, M., and Drusano, G.L. (2004). Selection of a moxifloxacin dose that suppresses drug resistance in Mycobacterium tuberculosis, by use of an in vitro pharmacodynamic infection model and mathematical modeling. J. Infect. Dis. *190*, 1642-1651. 10.1086/424849.
2. Cavaleri, M., and Manolis, E. (2015). Hollow Fiber System Model for Tuberculosis: The European Medicines Agency Experience. Clinical infectious diseases : an official publication of the Infectious Diseases Society of America *61 Suppl 1*, S1-4. 10.1093/cid/civ484.
3. European Medicines Agency Qualification Opinion In-vitro Hollow Fiber System Model of Tuberculosis (HSF-TB). (2015) https://www.fibercellsystems.com/wp-content/uploads/2022/11/Article-EMAEndorsement.pdf.
4. U.S. Food and Drug Administration (FDA). Pulmonary Tuberculosis: Developing Drugs for Treatment. Guidance Document (2022) https://www.fda.gov/media/164606/download.
5. Gloede, J., Scheerans, C., Derendorf, H., and Kloft, C. (2010). In vitro pharmacodynamic models to determine the effect of antibacterial drugs. J. Antimicrob. Chemother. *65*, 186-201. 10.1093/jac/dkp434.
6. Maitra, A., Solanki, P., Sadouki, Z., McHugh, T.D., and Kloprogge, F. (2021). Improving the Drug Development Pipeline for Mycobacteria: Modelling Antibiotic Exposure in the Hollow Fibre Infection Model. Antibiotics *10*. 10.3390/antibiotics10121515.
7. Drusano, G.L. (2017). Pre-clinical in vitro infection models. Curr. Opin. Pharmacol. *36*, 100-106. 10.1016/j.coph.2017.09.011.
8. Sadouki, Z., McHugh, T.D., Aarnoutse, R., Ortiz Canseco, J., Darlow, C., Hope, W., van Ingen, J., Longshaw, C., Manissero, D., Mead, A., et al. (2021). Application of the hollow fibre infection model (HFIM) in antimicrobial development: a systematic review and recommendations of reporting. J. Antimicrob. Chemother. *76*, 2252-2259. 10.1093/jac/dkab160.
9. Mason, A.B., and Dartois, V. (2021). Drug Sensitivity Testing of Mycobacterium tuberculosis Growing in a Hollow Fiber Bioreactor. Methods. Mol. Biol. *2314*, 715-731. 10.1007/978-1-0716-1460-0_31.
10. Gumbo, T., Pasipanodya, J.G., Romero, K., Hanna, D., and Nuermberger, E. (2015). Forecasting Accuracy of the Hollow Fiber Model of Tuberculosis for Clinical Therapeutic Outcomes. Clinical infectious diseases : an official publication of the Infectious Diseases Society of America *61 Suppl 1*, S25-31. 10.1093/cid/civ427.
11. Gumbo, T., Angulo-Barturen, I., and Ferrer-Bazaga, S. (2015). Pharmacokinetic-pharmacodynamic and dose-response relationships of antituberculosis drugs: recommendations and standards for industry and academia. J. Infect. Dis. *211 Suppl 3*, S96-S106. 10.1093/infdis/jiu610.
12. Kloprogge, F., Hammond, R., Kipper, K., Gillespie, S.H., and Della Pasqua, O. (2019). Mimicking in-vivo exposures to drug combinations in-vitro: anti-tuberculosis drugs in lung lesions and the hollow fiber model of infection. Sci. Rep. *9*, 13228. 10.1038/s41598-019-49556-5.
13. Wale, Y.M., Roberts, J.A., and Sime, F.B. (2024). Dynamic In Vitro PK/PD Infection Models for the Development and Optimisation of Antimicrobial Regimens: A Narrative Review. Antibiotics *13*. 10.3390/antibiotics13121201.
14. Heinrichs, M.T., Drusano, G.L., Brown, D.L., Maynard, M.S., Sy, S.K.B., Rand, K.H., Peloquin, C.A., Louie, A., and Derendorf, H. (2019). Dose optimization of moxifloxacin and linezolid against tuberculosis using mathematical modeling and simulation. Int. J. Antimicrob. Agents *53*, 275-283. 10.1016/j.ijantimicag.2018.10.012.
15. Singh, S., Gumbo, T., Boorgula, G.D., Thomas, T.A., Philley, J.V., and Srivastava, S. (2024). Omadacycline pharmacokinetics/pharmacodynamics and efficacy against

multidrug-resistant Mycobacterium tuberculosis in the hollow fiber system model. Antimicrob. Agents Chemother. *68*, e0108023. 10.1128/aac.01080-23.

16. Singh, S., Gumbo, T., Alffenaar, J.W., Boorgula, G.D., Shankar, P., Thomas, T.A., Dheda, K., Malinga, L., Raj, P., Aryal, S., and Srivastava, S. (2023). Meropenem-vaborbactam restoration of first-line drug efficacy and comparison of meropenem-vaborbactam-moxifloxacin versus BPaL MDR-TB regimen. Int. J. Antimicrob. Agents *62*, 106968. 10.1016/j.ijantimicag.2023.106968.
17. van Rijn, S.P., Srivastava, S., Wessels, M.A., van Soolingen, D., Alffenaar, J.C., and Gumbo, T. (2017). Sterilizing Effect of Ertapenem-Clavulanate in a Hollow-Fiber Model of Tuberculosis and Implications on Clinical Dosing. Antimicrob. Agents Chemother. *61*. 10.1128/AAC.02039-16.
18. Deshpande, D., Srivastava, S., Nuermberger, E., Pasipanodya, J.G., Swaminathan, S., and Gumbo, T. (2016). A Faropenem, Linezolid, and Moxifloxacin Regimen for Both Drug-Susceptible and Multidrug-Resistant Tuberculosis in Children: FLAME Path on the Milky Way. Clinical infectious diseases : an official publication of the Infectious Diseases Society of America *63*, S95-S101. 10.1093/cid/ciw474.
19. Srivastava, S., Deshpande, D., Magombedze, G., van Zyl, J., Cirrincione, K., Martin, K., Bendet, P., Berg, A., Hanna, D., Romero, K., et al. (2020). Duration of pretomanid/moxifloxacin/pyrazinamide therapy compared with standard therapy based on time-to-extinction mathematics. J. Antimicrob. Chemother. *75*, 392-399. 10.1093/jac/dkz460.
20. Gumbo, T., Chapagain, M., Magombedze, G., Srivastava, S., Deshpande, D., Pasipanodya, J.G., Gumbo, R., Dheda, K., Diacon, A., Hermann, D., and Hanna, D. (2022). Novel tuberculosis combination regimens of two and three-months therapy duration. Biorxiv. https://doi.org/10.1101/2022.03.13.484155.
21. Velkov, T., Bergen, P.J., Lora-Tamayo, J., Landersdorfer, C.B., and Li, J. (2013). PK/PD models in antibacterial development. Curr. Opin. Microbiol. *16*, 573-579. 10.1016/j.mib.2013.06.010.
22. Aguilar-Ayala, D.A., Sanz-Garcia, F., Rabodoarivelo, M.S., Susanto, B.O., Bailo, R., Eveque-Mourroux, M.R., Willand, N., Simonsson, U.S.H., Ramon-Garcia, S., Lucia, A., and consortium, E.T. (2024). Evaluation of critical parameters in the hollow-fibre system for tuberculosis: A case study of moxifloxacin. Br. J. Clin. Pharmacol. *90*, 1711-1727. 10.1111/bcp.16068.
23. Hollow Fiber System of Tuberculosis (HFS-TB): A Laboratory Manual to Guide System Engineering, Study Design and Execution. (2018). 1-30.
24. Silakari, O., and Singh, P.K. (2021). ADMET tools: Prediction and assessment of chemical ADMET properties of NCEs. Concepts and Experimental Protocols of Modelling and Informatics in Drug Design, 299-320. https://doi.org/10.1016/B978-0-12-820546-4.00014-3.
25. Pajouhesh, H., and Lenz, G.R. (2005). Medicinal chemical properties of successful central nervous system drugs. NeuroRx : the journal of the American Society for Experimental NeuroTherapeutics *2*, 541-553. 10.1602/neurorx.2.4.541.
26. Perveen, S., Kumari, D., Singh, K., and Sharma, R. (2022). Tuberculosis drug discovery: Progression and future interventions in the wake of emerging resistance. Eur. J. Med. Chem. *229*, 114066. 10.1016/j.ejmech.2021.114066.
27. Van der Paardt, A.L., Akkerman, O.W., Gualano, G., Palmieri, F., Davies Forsman, L., Aleksa, A., Tiberi, S., de Lange, W.C., Bolhuis, M.S., Skrahina, A., et al. (2017). Safety and tolerability of clarithromycin in the treatment of multidrug-resistant tuberculosis. Eur. Respir. J. *49*. 10.1183/13993003.01612-2016.
28. Conradie, F., Bagdasaryan, T.R., Borisov, S., Howell, P., Mikiashvili, L., Ngubane, N., Samoilova, A., Skornykova, S., Tudor, E., Variava, E., et al. (2022). Bedaquiline-Pretomanid-Linezolid Regimens for Drug-Resistant Tuberculosis. N. Engl. J. Med. *387*, 810-823. 10.1056/NEJMoa2119430.

29. Alfarisi, O., Alghamdi, W.A., Al-Shaer, M.H., Dooley, K.E., and Peloquin, C.A. (2017). Rifampin vs. rifapentine: what is the preferred rifamycin for tuberculosis? Expert review of clinical pharmacology *10*, 1027-1036. 10.1080/17512433.2017.1366311.
30. Deshkar, A.T., and Shirure, P.A. (2022). Bedaquiline: A Novel Diarylquinoline for Multidrug-Resistant Pulmonary Tuberculosis. Cureus *14*, e28519. 10.7759/cureus.28519.
31. Raaijmakers, J., Salillas, S., Aarnoutse, R., Svensson, E., Te Brake, L., Stemkens, R., Wertheim, H., Hoefsloot, W., and van Ingen, J. (2025). Bedaquiline does not enhance a clofazimine-azithromycin-ethambutol regimen against Mycobacterium avium in the hollow-fiber system. Antimicrob. Agents Chemother. *69*, e0146424. 10.1128/aac.01464-24.
32. Lounis, N., Vranckx, L., Gevers, T., Kaniga, K., and Andries, K. (2016). In vitro culture conditions affecting minimal inhibitory concentration of bedaquiline against M. tuberculosis. Med. Mal. Infect. *46*, 220-225. 10.1016/j.medmal.2016.04.007.
33. TB-Platform for the Aggregation of Preclinical Experiments Data (TB-APEX). (2024) https://c-path.org/tools-platforms/tb-apex/TB-Platform
34. Gumbo, T., Srivastava, S., Deshpande, D., Pasipanodya, J.G., Berg, A., Romero, K., Hermann, D., and Hanna, D. (2023). Hollow-fibre system model of tuberculosis reproducibility and performance specifications for best practice in drug and combination therapy development. J Antimicrob Chemother *78*, 953-964. 10.1093/jac/dkad029.
35. Al-Sallami, H.S., Cheah, S.L., Han, S.Y., Liew, J., Lim, J., Ng, M.A., Solanki, H., Soo, R.J., Tan, V., and Duffull, S.B. (2014). Between-subject variability: should high be the new normal? Eur. J. Clin. Pharmacol. *70*, 1403-1404. 10.1007/s00228-014-1740-8.
36. Drusano, G.L., Sgambati, N., Eichas, A., Brown, D.L., Kulawy, R., and Louie, A. (2010). The combination of rifampin plus moxifloxacin is synergistic for suppression of resistance but antagonistic for cell kill of Mycobacterium tuberculosis as determined in a hollow-fiber infection model. mBio *1*. 10.1128/mBio.00139-10.
37. Deshpande, D., Srivastava, S., Nuermberger, E., Pasipanodya, J.G., Swaminathan, S., and Gumbo, T. (2016). Concentration-Dependent Synergy and Antagonism of Linezolid and Moxifloxacin in the Treatment of Childhood Tuberculosis: The Dynamic Duo. Clin Infect Dis *63*, S88-S94. 10.1093/cid/ciw473.
38. Hou, Y., Mi, K., Sun, L., Zhou, K., Wang, L., Zhang, L., Liu, Z., and Huang, L. (2022). The Application of Hollow Fiber Cartridge in Biomedicine. Pharmaceutics *14*. 10.3390/pharmaceutics14071485.
39. C, H., AJ, L., and D, H. (1995). Exploring QSAR: Fundamentals and Applications in Chemistry and Biology. American Chemical Society. 10.1021/jm950902o.
40. Boorgula, G.D., Singh, S., Shankar, P., Gumbo, T., Heysell, S.K., and Srivastava, S. (2023). Isoniazid pharmacokinetics/pharmacodynamics as monotherapy and in combination regimen in the hollow fiber system model of Mycobacterium kansasii. Tuberculosis *138*, 102289. 10.1016/j.tube.2022.102289.
41. Park, Y., Tung, P.M., Anh, N.K., Cho, Y.S., and Shin, J.G. (2024). Application of the Hollow-Fiber Infection Model to Personalized Precision Dosing of Isoniazid in a Clinical Setting. J. Korean Med. Sci. *39*, e104. 10.3346/jkms.2024.39.e104.
42. Tao, M., Liu, F., and Xue, L. (2012). Hydrophilic poly(vinylidene fluoride) (PVDF) membrane by in situ polymerisation of 2-hydroxyethyl methacrylate (HEMA) and micro-phase separation. J. Mater. Chem. *22*. 10.1039/c2jm30695f.
43. Etale, A., Onyianta, A.J., Turner, S.R., and Eichhorn, S.J. (2023). Cellulose: A Review of Water Interactions, Applications in Composites, and Water Treatment. Chem. Rev. *123*, 2016-2048. 10.1021/acs.chemrev.2c00477.
44. Long, H.P., Lai, C.C., and Chung, C.K. (2016). Polyethylene glycol coating for hydrophilicity enhancement of polydimethylsiloxane self-driven microfluidic chip. Surf. Coat. Technol. *320*, 315-319. 10.1016/j.surfcoat.2016.12.059.
45. Wang, L., Wei, J., and Wu, B. (2016). Enhancing hydrophilicity performance of polysulfone hollow fiber membrane by surface modification via UV-induced graft polymerization of HEA. Desalination Water Treat. *57*, 16269-16276.

46. Said, N., Hasbullah, H., Ismail, A.F., Othman, M.H.D., Goh, P.S., Zainol Abidin, M.N., ..., and & Ng, B.C. (2017). Enhanced hydrophilic polysulfone hollow fiber membranes with addition of iron oxide nanoparticles. Polym. Int. *66*, 1424-1429.
47. Peechmani, P., Othman, M.H.D., Kamaludin, R., Puteh, M.H., Jaafar, J., Rahman, M.A., ..., and & Djuli, S.M. (2021). High flux polysulfone braided hollow fiber membrane for wastewater treatment role of zinc oxide as hydrophilic enhancer. J. Environ. Chem. Eng. *9*, 105873.
48. Yoo, S.M., and Ghosh, R. (2018). A method for coating of hollow fiber membranes with calcium alginate. J. Membr. Sci. *558*, 45-51. 10.1016/j.memsci.2018.04.044.
49. Stadler, J.A.M., Maartens, G., Meintjes, G., and Wasserman, S. (2023). Clofazimine for the treatment of tuberculosis. Front. Pharmacol. *14*, 1100488. 10.3389/fphar.2023.1100488.
50. Jayaram, R., Shandil, R.K., Gaonkar, S., Kaur, P., Suresh, B.L., Mahesh, B.N., Jayashree, R., Nandi, V., Bharath, S., Kantharaj, E., and Balasubramanian, V. (2004). Isoniazid pharmacokinetics-pharmacodynamics in an aerosol infection model of tuberculosis. Antimicrob. Agents Chemother. *48*, 2951-2957. 10.1128/AAC.48.8.2951-2957.2004.
51. Gumbo, T., Louie, A., Deziel, M.R., Liu, W., Parsons, L.M., Salfinger, M., and Drusano, G.L. (2007). Concentration-dependent Mycobacterium tuberculosis killing and prevention of resistance by rifampin. Antimicrob. Agents Chemother. *51*, 3781-3788. 10.1128/AAC.01533-06.
52. Mallikaarjun, S., Chapagain, M.L., Sasaki, T., Hariguchi, N., Deshpande, D., Srivastava, S., Berg, A., Hirota, K., Inoue, Y., Matsumoto, M., et al. (2020). Cumulative Fraction of Response for Once- and Twice-Daily Delamanid in Patients with Pulmonary Multidrug-Resistant Tuberculosis. Antimicrob. Agents Chemother. *65*. 10.1128/AAC.01207-20.
53. Beraldi-Magalhaes, F., Parker, S.L., Sanches, C., Sousa Garcia, L., Souza Carvalho, B.K., Fachi, M.M., de Liz, M.V., Pontarolo, R., Lipman, J., Cordeiro-Santos, M., and Roberts, J.A. (2021). Is Dosing of Ethambutol as Part of a Fixed-Dose Combination Product Optimal for Mechanically Ventilated ICU Patients with Tuberculosis? A Population Pharmacokinetic Study. Antibiotics *10*. 10.3390/antibiotics10121559.
54. Ahmad, Z., Peloquin, C.A., Singh, R.P., Derendorf, H., Tyagi, S., Ginsberg, A., Grosset, J.H., and Nuermberger, E.L. (2011). PA-824 exhibits time-dependent activity in a murine model of tuberculosis. Antimicrob. Agents. Chemother. *55*, 239-245. 10.1128/AAC.00849-10.
55. Bateson, A., Ortiz Canseco, J., McHugh, T.D., Witney, A.A., Feuerriegel, S., Merker, M., Kohl, T.A., Utpatel, C., Niemann, S., Andres, S., et al. (2022). Ancient and recent differences in the intrinsic susceptibility of Mycobacterium tuberculosis complex to pretomanid. J. Antimicrob. Chemother. *77*, 1685-1693. 10.1093/jac/dkac070.
56. Cadwell, J. (2015). The Hollow Fiber Infection Model: Principles and Practice. Adv Antibiotics Antibodies *1:1*. 10.4172/aaa.1000101.
57. Omar, S.V., Ismail, F., Ndjeka, N., Kaniga, K., and Ismail, N.A. (2022). Bedaquiline-Resistant Tuberculosis Associated with Rv0678 Mutations. N. Engl. J. Med. *386*, 93-94. 10.1056/NEJMc2103049.
58. Rodriguez-Ochoa, J.L., Sauco-Carballo, C., Perez-Palacios, P., Merino-Bohorquez, V., Velazquez-Escudero, A., Lopez-Cerero, L., Rodriguez-Bano, J., Rodriguez-Martinez, J.M., Pascual, A., and Docobo-Perez, F. (2025). Pharmacokinetic/pharmacodynamic optimization of temocillin treatment against CTX-M-15-producing Klebsiella pneumoniae isolates in a hollow-fiber infection model. Antimicrob. Agents Chemother., e0094625. 10.1128/aac.00946-25.
59. van Heeswijk, R.P., Dannemann, B., and Hoetelmans, R.M. (2014). Bedaquiline: a review of human pharmacokinetics and drug-drug interactions. J. Antimicrob. Chemother. *69*, 2310-2318. 10.1093/jac/dku171.
60. Alghamdi, W.A., Al-Shaer, M.H., Kipiani, M., Barbakadze, K., Mikiashvili, L., Kempker, R.R., and Peloquin, C.A. (2021). Pharmacokinetics of bedaquiline, delamanid and clofazimine in patients with multidrug-resistant tuberculosis. J. Antimicrob. Chemother. *76*, 1019-1024. 10.1093/jac/dkaa550.

61. Moodliar, R., Aksenova, V., Frias, M.V.G., van de Logt, J., Rossenu, S., Birmingham, E., Zhuo, S., Mao, G., Lounis, N., Kambili, C., and Bakare, N. (2021). Bedaquiline for multidrug-resistant TB in paediatric patients. Int. J. Tuberc. Lung Dis. *25*, 716-724. 10.5588/ijtld.21.0022.
62. Svensson, E.M., Dosne, A.G., and Karlsson, M.O. (2016). Population Pharmacokinetics of Bedaquiline and Metabolite M2 in Patients With Drug-Resistant Tuberculosis: The Effect of Time-Varying Weight and Albumin. CPT Pharmacometrics Syst. Pharmacol. *5*, 682-691. 10.1002/psp4.12147.
63. Stephens, R.H., Benjamin, A.R., and Walters, D.V. (1996). Volume and protein concentration of epithelial lining liquid in perfused in situ postnatal sheep lungs. J. Appl. Physiol. *80*, 1911-1920. 10.1152/jappl.1996.80.6.1911.
64. Ngwalero, P., Brust, J.C.M., van Beek, S.W., Wasserman, S., Maartens, G., Meintjes, G., Joubert, A., Norman, J., Castel, S., Gandhi, N.R., et al. (2021). Relationship between Plasma and Intracellular Concentrations of Bedaquiline and Its M2 Metabolite in South African Patients with Rifampin-Resistant Tuberculosis. Antimicrob. Agents Chemother. *65*, e0239920. 10.1128/AAC.02399-20.
65. Guay, D.R., Gustavson, L.E., Devcich, K.J., Zhang, J., Cao, G., and Olson, C.A. (2001). Pharmacokinetics and tolerability of extended-release clarithromycin. Clin. Ther. *23*, 566-577. 10.1016/s0149-2918(01)80060-6.
66. Ramirez, G., Pham, A.C., Clulow, A.J., Salim, M., Hawley, A., and Boyd, B.J. (2021). Sustained absorption of delamanid from lipid-based formulations as a path to reduced frequency of administration. Drug. Deliv. Transl. Res. *11*, 1236-1244. 10.1007/s13346-020-00851-z.
67. Bekker, A., Schaaf, H.S., Draper, H.R., van der Laan, L., Murray, S., Wiesner, L., Donald, P.R., McIlleron, H.M., and Hesseling, A.C. (2016). Pharmacokinetics of Rifampin, Isoniazid, Pyrazinamide, and Ethambutol in Infants Dosed According to Revised WHO-Recommended Treatment Guidelines. Antimicrob. Agents. Chemother. *60*, 2171-2179. 10.1128/AAC.02600-15.
68. Tikiso, T., McIlleron, H., Abdelwahab, M.T., Bekker, A., Hesseling, A., Chabala, C., Davies, G., Zar, H.J., Rabie, H., Andrieux-Meyer, I., et al. (2022). Population pharmacokinetics of ethambutol in African children: a pooled analysis. J. Antimicrob. Chemother. *77*, 1949-1959. 10.1093/jac/dkac127.
69. Lee, C.S., Brater, D.C., Gambertoglio, J.G., and Benet, L.Z. (1980). Disposition kinetics of ethambutol in man. J. Pharmacokinet. Biopharm. *8*, 335-346. 10.1007/BF01059382.
70. Srivastava, S., Musuka, S., Sherman, C., Meek, C., Leff, R., and Gumbo, T. (2010). Efflux-pump-derived multiple drug resistance to ethambutol monotherapy in Mycobacterium tuberculosis and the pharmacokinetics and pharmacodynamics of ethambutol. J. Infect. Dis. *201*, 1225-1231. 10.1086/651377.
71. Ginsburg, A.S., Lee, J., Woolwine, S.C., Grosset, J.H., Hamzeh, F.M., and Bishai, W.R. (2005). Modeling in vivo pharmacokinetics and pharmacodynamics of moxifloxacin therapy for Mycobacterium tuberculosis infection by using a novel cartridge system. Antimicrob. Agents Chemother. *49*, 853-856. 10.1128/AAC.49.2.853-856.2005.
72. Kim, M.K., and Nightingale, C.H. (2000). Pharmacodynamics and pharmacokinetics of the fluoroquinolones. In V. T. Andriole (ed.), The quinolones, 3rd ed., 169-202.
73. Lyons, M.A. (2018). Modeling and Simulation of Pretomanid Pharmacokinetics in Pulmonary Tuberculosis Patients. Antimicrob. Agents Chemother. *62*. 10.1128/AAC.02359-17.
74. Liu, Y., Tan, Y., Wei, G., Lu, Z., Liu, Y., Yang, B., Hui, A.M., and Li, K. (2022). Safety and pharmacokinetic profile of pretomanid in healthy Chinese adults: Results of a phase I single dose escalation study. Pulm. Pharmacol. Ther. *73-74*, 102132. 10.1016/j.pupt.2022.102132.
75. Mehta, K., Guo, T., van der Graaf, P.H., and van Hasselt, J.G.C. (2023). Predictions of Bedaquiline and Pretomanid Target Attainment in Lung Lesions of Tuberculosis Patients using Translational Minimal Physiologically Based Pharmacokinetic Modeling. Clin. Pharmacokinet. *62*, 519-532. 10.1007/s40262-023-01217-7.

76. Karakitsios, E., Della Pasqua, O., and Dokoumetzidis, A. (2025). Extrapolation of lung pharmacokinetics of bedaquiline across species using physiologically-based pharmacokinetic modelling. Br. J. Clin. Pharmacol. *91*, 3167-3178. 10.1002/bcp.70163.
77. Mehta, K., Guo, T., van der Graaf, P.H., and van Hasselt, J.G.C. (2024). Model-based dose optimization framework for bedaquiline, pretomanid and linezolid for the treatment of drug-resistant tuberculosis. Br. J. Clin. Pharmacol. *90*, 463-474. 10.1111/bcp.15925.
78. Stott, K.E., Pertinez, H., Sturkenboom, M.G.G., Boeree, M.J., Aarnoutse, R., Ramachandran, G., Requena-Mendez, A., Peloquin, C., Koegelenberg, C.F.N., Alffenaar, J.W.C., et al. (2018). Pharmacokinetics of rifampicin in adult TB patients and healthy volunteers: a systematic review and meta-analysis. J. Antimicrob. Chemother. *73*, 2305-2313. 10.1093/jac/dky152.
79. Clewe, O., Goutelle, S., Conte, J.E., Jr., and Simonsson, U.S. (2015). A pharmacometric pulmonary model predicting the extent and rate of distribution from plasma to epithelial lining fluid and alveolar cells--using rifampicin as an example. Eur. J. Clin. Pharmacol. *71*, 313-319. 10.1007/s00228-014-1798-3.
80. European Medicines Agency. Investigation of bioequivalence - Scientific guideline. Available online. (2010).

## STAR★METHODS

### METHOD DETAILS

**Culture media and drugs**. Unless otherwise stated, Middlebrook 7H9 broth (Becton Dickinson, New Jersey, USA) supplemented with 10% (vol/vol) Middlebrook oleic acid-albumin-dextrose-catalase (OADC) (Becton Dickinson, New Jersey, USA), 0.5% (vol/vol) glycerol (Scharlau, Hamburg, Germany) and 0.05% (vol/vol) tyloxapol (Sigma-Aldrich, St. Louis, USA) (from now on abbreviated as 7H9/OADC/Gly/Tx) or Middlebrook 7H9 broth supplemented with 0.0004% (vol/vol) cholesterol (Sigma-Aldrich, St. Louis, USA), dissolved in ethanol:tyloxapol mixture 1:1, 0.085% (vol/vol) NaCl (PanReac Química S.L.U., Barcelona, Spain) and 0.0004% (vol/vol) catalase (Sigma-Aldrich, St. Louis, USA) (from now on abbreviated as 7H9/Chol/NaCl/Cat) were used at 37ºC without $CO_2$.

EMB, INH, MXF (European Pharmacopeia Reference Standard I0500000, E1850000 and Y0000703, respectively) and LZD (Sigma-Aldrich, St. Louis, USA, USP Reference Standard 1367561) were dissolved in sterile water on the day of starting the experiment. RMP (European Pharmacopeia Reference Standard, R0700000), RPT, CLA (Sigma-Aldrich, St. Louis, USA, R0533-25MG and A3487-100MG, respectively), BDQ, PTD (RTI International/TB Alliance, FF07153068 and 11356-156, respectively) and DLM (MedChemExpress, New Jersey, USA, HY-10846/CS-5866) were dissolved in dimethyl sulfoxide on the day of starting the experiment. When needed, freshly prepared stock solutions were frozen and thawed once after a maximum of four days at -20ºC for single use. Drug aliquots were diluted to the required concentration in 7H9/OADC/Gly/Tx or 7H9/Chol/NaCl/Cat (in the case of INH and the optimization approaches with BDQ and BPaL) and used immediately. Bioanalyses included a drug stock control and the syringe's

872 solution, which contained the compound dissolved in broth media. Except for PTD-PS
873 and PTD-cellulose compatibility tests' syringes, and the one containing LZD for the
874 BPaL approach, these controls barely diverged from their theoretical concentrations.
875 When this occurred, expected concentrations and PK parameters were recalculated,
876 thereby not affecting conclusions from compatibility assessments. They were prepared
877 before the freeze-thaw cycle of the samples and analyzed after that, which validates the
878 stability of the drugs in these conditions.

879 **HFS experimental set up**. A schematic depiction of the HFS-TB can be found in **Figure**
880 **S1**. Materials, technical specifications and HFS-TB assembly is described by Aguilar-
881 Ayala DA, *et al*. [22]. Medium-size PS, PVDF and cellulose (FiberCell Systems, New
882 Market, USA. Refs C2011, C7011 and C8008, respectively) cartridges were used in this
883 study. Bottles, caps, tubing, fittings, filters and media were autoclaved before each assay.
884 As a sterility test, culture media was incubated first at 37ºC for 2 days and, then, at room
885 temperature for 2 additional days. On the day the HFS was assembled, the peristaltic
886 pump was switched on at a high rate to ensure there were no leakages throughout the
887 circuit. In compliance with manufacturer's recommendations (FiberCell Systems, New
888 Market, USA), Duet pumps were set at a rate of 25 U (~100-110 mL/min) to promote fast
889 distribution and equilibration of broth media and drug between the ICS and the ECS. HFS
890 compatibility tests included a pre-conditioning step of 3-4 days recirculating broth, so as
891 to accurately hydrate the fibers. Total volume of the HFS was 200 mL. Before each
892 sampling, the ECS content was thoroughly mixed through the cartridge ports using 3-
893 bodies Luer-Lock syringes of 20 mL (BBraun, Melsungen, Germany). The same 20 mL
894 syringes, or 30 mL ones (Rays, Osimo, Italy), were used for drug administration.
895 Compound concentrations within syringes and pump settings are enclosed in **Table S5**.
896 Polypropylene 3-bodies Luer-Lock 1 mL syringes (Thermofisher Scientific, Waltham,

USA) were used for sampling. Regarding the optimization approach for BDQ and BPaL, previous data on binding to plastic -especially polypropylene- and silicone were taken into account [31,32]. Therefore, 1/16" and 3/16" ID polycarbonate fittings (Masterflex, Gelsenkirchen, Germany), 3-bodies Luer-Lock 20 mL (SAI Infusion Technologies, Lake Villa, USA) and 1 mL (BD, Becton Dickinson, New Jersey, USA) polycarbonate syringes, glass tubes and polystyrene plates (TPP®, Trasadingen, Switzerland) were used in these experiments. PK samples were stored at -80 ºC until quantification.

Syringe and peristaltic pumps rates were obtained using standard PK equations. The elimination rate constant (k) was calculated based on **equation 1**: $k = ln(2)/T_{1/2}$, where $T_{1/2}$ is the half-life of the drug under study. The clearance (CL) was derived according to **equation 2**: $CL = k \cdot V$, where V is the total volume of the system (200 mL). The compound concentration at time (t) after infusion ($C_t$) was obtained using **equation 3**: $C_t = C_S \cdot e^{-kt}$, where $C_S$ is the concentration in the infusion syringe divided by the clearance.

**Mimicking a pharmacokinetic profile in the HFS for drug-fiber compatibility tests**. Drug-fiber compatibility tests consist in infusing a compound into the system -in absence of bacteria- to mimic a specific PK profile and gauging the drug concentration in the system over time. There are two alternatives to address this assay: on the one hand, a known concentration of the antibiotic is infused into the HFS-TB so as to reach $C_{max}$ at the targeted $T_{max}$, and the system is kept static for 1.5-2 hours before drug dilution. On the other hand, a clinically plausible PK profile of more than one dose is simulated. In both approaches, drug binding is spotted if target concentrations are not achieved and/or they vary between compartments.

In this study, we mainly centered on the second approach; thereby mimicking PK profiles resembling the *in vivo* context for *M. tuberculosis* therapy: i.e., drug free concentrations (unbound to proteins) in the site of infection (lungs), as long as these data were available.

A summary of target PK parameters is encompassed in **Table 4**. A 3 days QD (*quaque die*; once a day) dosing was designed for all drugs except for CLA (3 days QAD; *quaque altera die*: every other day), DLM (4 days BID; *bis in die*: twice a day) and BDQ (3 days; single dose). In each case, the drug was infused into the system at a rate and concentration that led to the steady state $C_{max}$ ($C_{max, ss}$) at the predetermined $T_{max}$. In the case of BDQ, $C_{max, ss}$ was maintained for 1.5 hours before drug dilution. In all cases, drug clearance was set at the corresponding rate (see afore-mentioned equation), and ca. 15 time points were sampled from both the ICS and the ECS.

A drug was deemed within the compatibility range with a specific cartridge when the following criteria were met in the ECS: $AUC_{0\text{-}24h, real}/AUC_{0\text{-}24h, expected}$ ($AUC_{0\text{-}24h, ECS, ratio}$) = 0.8-1.25; $C_{max, ss, real}/C_{max, ss, expected}$ ($C_{max, ss, ECS, ratio}$) = 0.7-1.3, and $T_{1/2, real}/T_{1/2, expected}$ ($T_{1/2, ECS, ratio}$) = 0.6-1.4, based on EMA bioequivalence guidelines [80], as well as the convention on acceptable coefficients of variation in between-subject variance of PK parameters, extracted from Al-Sallami HS, *et al* [35]. If these criteria were not met, a drug was considered outside the compatibility range with a specific cartridge.

**Optimization approach to mimic a pharmacokinetic profile of bedaquiline in the HFS-TB.** As a proof of concept to optimize the use of highly lipophilic molecules in the HFS-TB, a median concentration at protein-unbound clinical steady state ($C_{med, ss}$) in the lung was targeted for BDQ (200 mg TIW; three times a week) (**Table 4**). To obtain that value, we followed the same procedure described by Raaijmakers J, *et al.* [31], taking into consideration BDQ's average plasma concentrations [60,61,64], protein binding [59] and plasma/lung ratio of albumin [62,63]. To keep $C_{med, ss}$ along 3 days in the ECS, six infusions a day of BDQ (1.65 mL/min of a 100 µg/mL syringe stock on the first day, and 1.65 mL/min of a 50 µg/mL syringe stock on the second and third days) were administered directly into the ECS ($T_{max}$ = 1 min). These values were calculated based on data from

947 BDQ's compatibility tests and the TB-APEX [33]. Drug clearance was set at an arbitrary
948 rate (corresponding to $T_{1/2}$ = 14.6 h; see afore-mentioned equation) and 19 time points
949 were sampled from the ECS.

950 **Optimization approach to mimic a pharmacokinetic profile of bedaquiline-**
951 **pretomanid-linezolid (BPaL) combination in the HFS-TB.** A 3-days unbound PK
952 profile of BDQ, PTD and LZD in lung was targeted in the HFS-TB (**Table 4)**. An
953 unbound $C_{med, ss}$ in the lung was aimed for BDQ in a cellulose cartridge, following a
954 slightly modified version of the infusions' schedule detailed above. Data from BDQ alone
955 in cellulose fibers was used to inform the design of the combination experiment (1.65
956 mL/min of a 20 µg/mL syringe stock on the first day, and 1.65 mL/min of a 10 µg/mL
957 syringe stock on the second and third days; $T_{max}$ = 1 min). PTD's PK profile was aimed
958 by adding thrice the amount of drug into the ICS in each infusion (**Table S5**). This was
959 done to counteract the unspecific binding registered from experiments with PTD alone in
960 cellulose fibers. Plus, five top-up infusions a day of PTD (1.20 mL/min of a 400 µg/mL
961 syringe stock; $T_{max}$ = 1 h) were administered to compensate its profile under LZD's
962 clearance, which held a shorter half-life (**Table 4**). 22 time points were sampled only
963 from the ECS, because it is the compartment where bacteria will be housed in PKPD
964 experiments and where BDQ was added, thereby assuming that BDQ's levels in the ICS
965 would be negligible.

966 **Preparation of drug samples and drug quantification**. A seven-point calibration curve
967 covering the range of expected drug concentrations in the experiment was established in
968 duplicate under the same matrix composition as the samples to be quantified.

969 The LC analysis was performed using a UPLC Acquity I-Class system (Waters®,
970 Milford, USA) equipped with an Acquity Ethylene Bridge Hybrid (BEH) C18 analytical
971 column (1.7 µm, 50 mm·2.1 mm). The mobile phase consisted of 5 mM ammonium

formate in water (phase A) or in acetonitrile (phase B) and the elution was performed with a 4 min gradient from 2% to 98% phase B, with an injection volume of 1 µL and a flow rate set at 600 µL/min. The UPLC system was coupled online to a Xevo TQD system (Waters®, Milford, USA) equipped with an ESI source. The mass spectrometer was operated in positive ion mode with a specific Multiple Reaction Monitoring (MRM) method for each compound (**Table S6**). The raw data were processed within the MassLynx software version 4.2 (Waters®, Milford, USA). In addition, bioanalytical LC-MS/MS methods for the compounds were validated for: i) selectivity and specificity -optimized LC-MSMS method with specific MRM transitions for each drug- (**Table S6**), ii) accuracy and precision -based on the $R^2$ values obtained for each calibration curves models-, iii) recovery -barely a difference between the expected and the calculated concentrations- and, iv) matrix effect -calibration curves built using the broth to mimic the samples to quantify-.

## QUANTIFICATION AND STATISTICAL ANALYSIS

Accuracy and precision of the calibration curves for drug quantification -0.3 nM to 500 or 1000 nM, depending on the range of expected concentrations- were evaluated based on $R^2$ values of linear regression (≥0.95). Each point of said curves was performed in duplicate. Accuracy of the $T_{1/2}$ calculated for drug clearance after each dose (2-3, depending on the targeted PK) was evaluated based on $R^2$ values of exponential regression (≥0.95).

## SUPPLEMENTAL INFORMATION

**Table S1.** Expected and measured concentrations from drug-fiber compatibility tests in the HFS-TB.

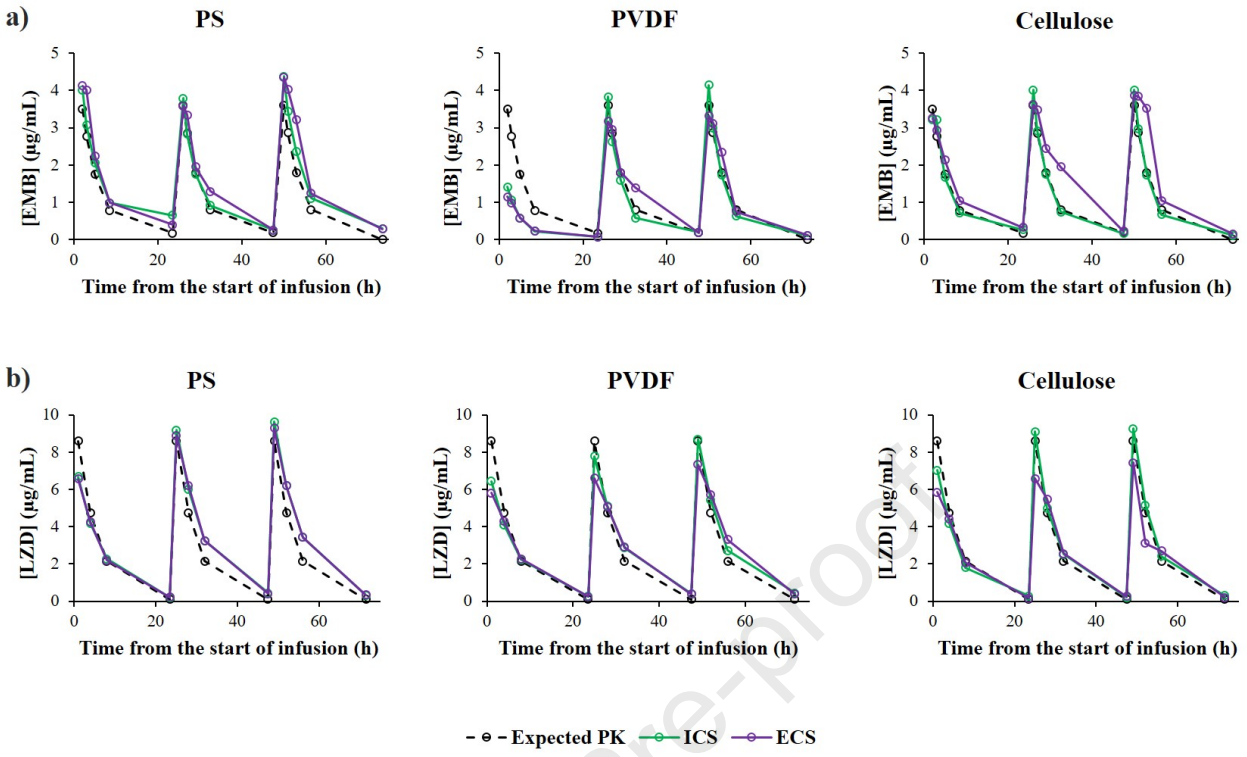

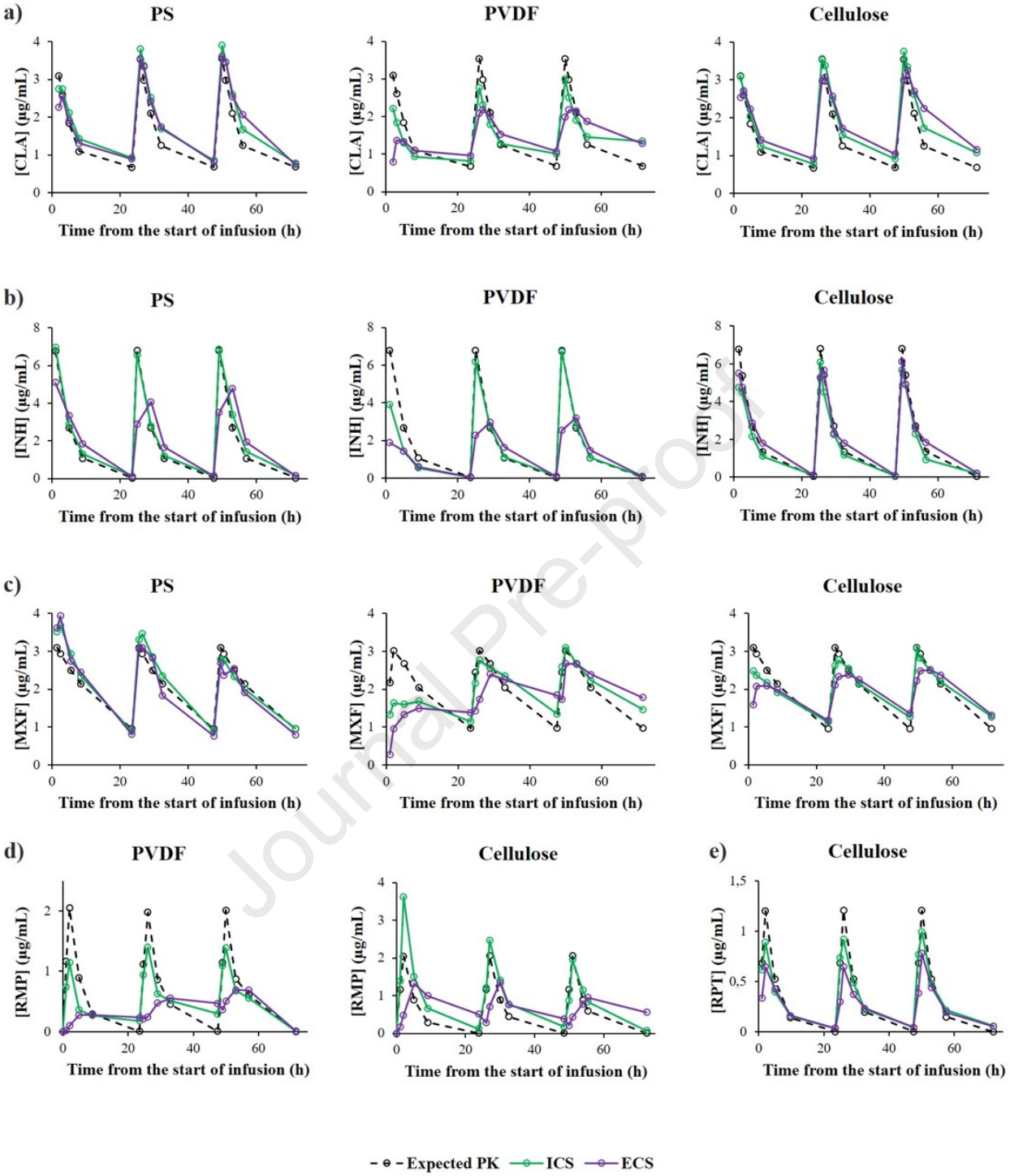

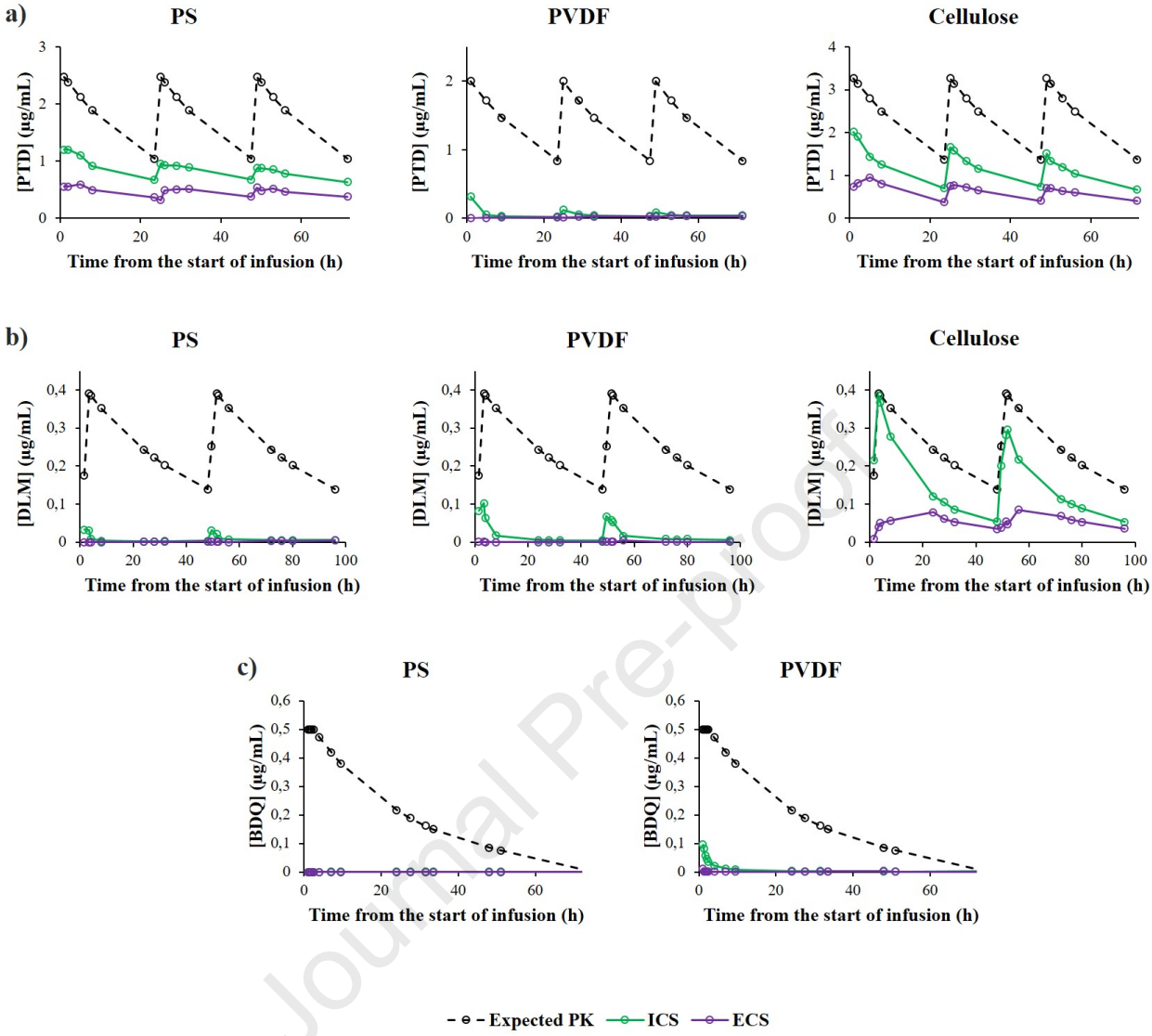

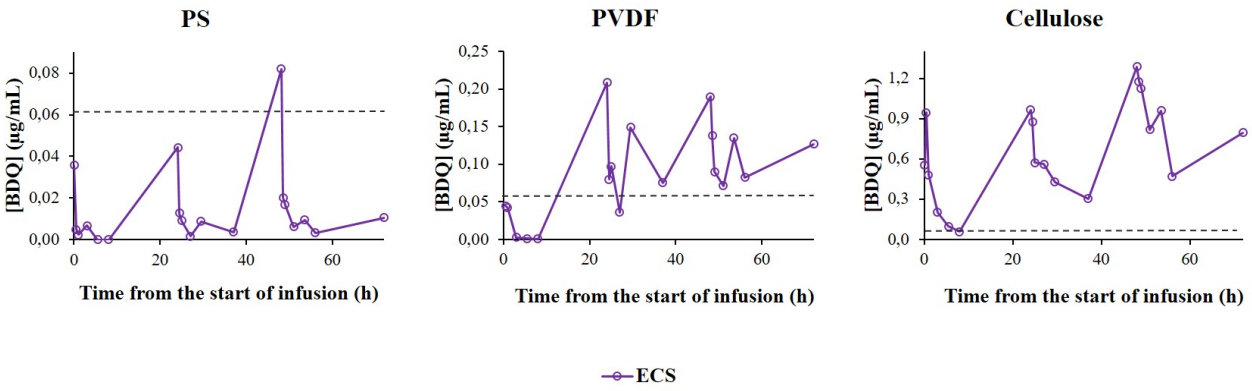

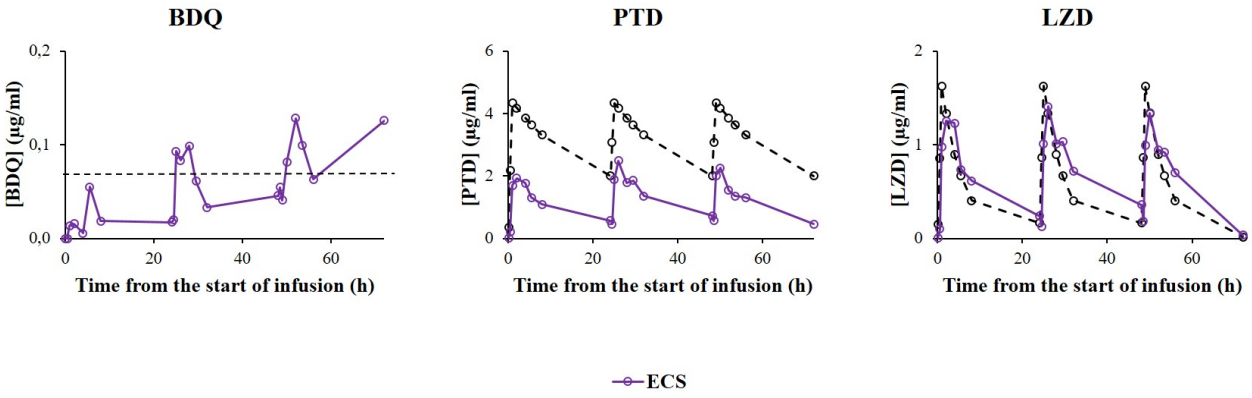

| Drug | Polysulfone | PVDF | Cellulose |
|---|---|---|---|
| INH | | | |
| EMB | | | |
| LZD | | | |
| RMP | | | |
| MXF | | | |
| CLA | | | |
| RPT | ND | ND | |
| PTD | | | |
| DLM | | | |
| BDQ | | | * |

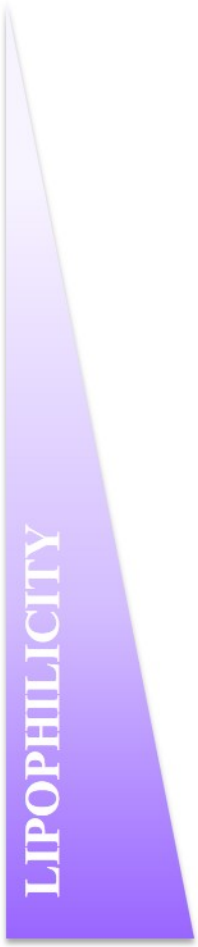


| Within the compatibility range | Outside the compatibility range (optimizable) | Outside the compatibility range |
|---|---|---|

- A comprehensive assay toolkit for the HFS-TB is provided.
- Polysulfone and cellulose fibers are the most suitable for compounds in the toolkit.
- A strategy to mimic BPaL exposure in the HFS-TB has been successfully implemented.
- Assessing drug concentrations in the extra-capillary space is a key verification step.

## KEY RESOURCES TABLE

| REAGENT OR RESOURCE | SOURCE | IDENTIFIER |
|---|---|---|
| **Chemicals, peptides, and recombinant proteins** | | |
| Middlebrook 7H9 broth | Becton Dickinson | Cat# 271310 |
| Middlebrook oleic acid-albumin-dextrose-catalase | Becton Dickinson | Cat# 212351 |
| Glycerol | Scharlau | Cat# 15523-1L-M |
| Tyloxapol | Sigma-Aldrich | Cat# T8761-50G |
| Cholesterol | Sigma-Aldrich | Cat# C3045-25 G |
| NaCl | Panreac Química S.L.U. | Cat# S1679 |
| Catalase | Sigma-Aldrich | Cat# C40-500MG |
| Ethambutol | European Pharmacopeia Reference Standard | Cat# I0500000 |
| Isoniazid | European Pharmacopeia Reference Standard | Cat# E1850000 |
| Moxifloxacin | European Pharmacopeia Reference Standard | Cat# Y0000703 |
| Linezolid | Sigma-Aldrich | Cat# 1367561 |
| Rifampicin | European Pharmacopeia Reference Standard | Cat# R0700000 |
| Rifapentine | Sigma-Aldrich | Cat# R0533-25MG |
| Clarithromycin | Sigma-Aldrich | Cat# A3487-100MG |
| Bedaquiline | RTI International/TB Alliance | Cat# FF07153068 |
| Pretomanid | RTI International/TB Alliance | Cat# 11356-156 |
| Delamanid | MedChemExpress | Cat# HY-10846/CS-5866 |
| Dimethyl sulfoxide | Sigma-Aldrich | Cat# 276855 |
| **Software and algorithms** | | |
| MassLynx software version 4.2 | Waters | NA |
| **Other** | | |
| Medium-size polysulfone cartridges | FiberCell Systems | Cat# C2011 |
| Medium-size polyvinylidene fluoride cartridges | FiberCell Systems | Cat# C7011 |
| Medium-size cellulose cartridges | FiberCell Systems | Cat# C8008 |
| 250 mL polycarbonate bottles | VWR | Cat# VWRI215-2204 |
| 4 L polycarbonate bottles | VWR | Cat# DS2205 -0010 |
| PKPD reservoir cap | FiberCell Systems | Cat# A1007 |
| Reservoir cap | FiberCell Systems | Cat# A1006 |
| Silicone pump tubing | Masterflex | Cat# 96410-16 |
| Polytetrafluoroethylene-based, hydrophobic filter unit | Millex-FG | Cat# SLFG05010 |
| C-flex tubing 0.8 mm ID | Masterflex | Cat# 06427-13 |
| C-flex tubing 1.6 mm ID | Masterflex | Cat# 06427-14 |
| BPT tubing 1.52” ID | Ismatec Saint-Gobain Pharmed BTP, Masterflex | Cat# S0732 |
| Polypropylene female Luer-lock fittings 1/16” ID | Masterflex | Cat# 14845571 |
| Polypropylene male Luer-lock fittings 1/16” ID | Masterflex | Cat# 13546720 |
| Polypropylene female Luer-lock fittings 3/16” ID | Masterflex | Cat# 15296618 |

| | | |
|---|---|---|
| Polypropylene male Luer-lock fittings 3/16” ID | Masterflex | Cat# 14860962 |
| Polycarbonate female Luer-lock fittings 1/16” ID | Masterffex | Cat# 12197750 |
| Polycarbonate male Luer-lock fittings 1/16” ID | Masterflex | Cat# 15819911 |
| Polycarbonate female Luer-lock fittings 3/16” ID | Masterffex | Cat# 15216088 |
| Polycarbonate male Luer-lock fittings 3/16” ID | Masterflex | Cat# 13538810 |
| Sterile polyamide microcrystalline T-joints | BBraun | Cat# 16494C |
| Clave needle-free connectors | Icumedical | Cat# 011-C1000 |
| Duet pumps | FiberCell Systems | Cat# P3202 |
| Peristaltic Ismatec Reglo pumps | Masterflex | Cat# ISM4408 |
| Masterflex LS pumps | Masterflex | Cat# 07522-30 |
| One Channel Programmable Syringe Pumps | New Era Pump Systems, Inc. | Cat# NE-1000 |
| Polypropylene 3-bodies Luer-Lock syringes of 20 mL | BBraun | Cat# 4617207V |
| Polypropylene 3-bodies Luer-Lock syringes of 30 mL | Rays | Cat# 30LL |
| Polypropylene 3-bodies Luer-Lock syringes of 1 mL | Thermo Scientific | Cat# 309628 |
| Polycarbonate 3-bodies Luer-Lock syringes of 20 mL | SAI Infusion Technologies | Cat# 847.356.0321 |
| Polycarbonate 3-bodies Luer-Lock syringes of 1 mL | Becton Dickinson | Cat# 309628 |
| Polystyrene p96-well plates | TPP | Cat# 92096 |
| TB-Platform for the Aggregation of Preclinical Experiments Data (TB-APEX) | NA | NA |